We are IntechOpen,
the world's leading publisher of
Open Access books
Built by scientists, for scientists

6,900
Open access books available

185,000
International authors and editors

200M
Downloads

154
Countries delivered to

Our authors are among the

TOP 1%
most cited scientists

12.2%
Contributors from top 500 universities

BOOK CITATION INDEX
CLARIVATE ANALYTICS
INDEXED

WEB OF SCIENCE™

Selection of our books indexed in the Book Citation Index
in Web of Science™ Core Collection (BKCI)

Interested in publishing with us?
Contact book.department@intechopen.com

Numbers displayed above are based on latest data collected.
For more information visit www.intechopen.com

Exergy and Environmental Considerations in Gas Turbine Technology and Applications

Richard 'Layi Fagbenle
BSME, PhD (Illinois), MSME(Iowa State),
USA

1. Introduction

Global CO_2 emissions by sector in 1990 for transportation, electric power, buildings, synfuels & hydrogen production, and industry were 20%, 27%, 15%, 0% and 38% respectively *[IPIECA Workshop, Baltimore, USA, 12-13 October 2004]*. In a 2095 scenario limiting the GHG to 550 ppm CO_2, the sectoral CO_2 emissions for transportation, electric power, buildings, synfuels & hydrogen production, and industry are 40%, 23%, 19%, 1% and 17% respectively *[IPIECA Workshop, Baltimore, USA, 12-13 October 2004]*. It is argued that the high cost of alternatives, and the strong demand for mobility, limits the effects of climate policies on the transportation sector, while more cost-effective emission reductions are found in the electric power and the industry sectors *[IPIECA Workshop, Baltimore, USA, 12-13 October 2004]*. While it is noted that climate change scenarios are replete with assumptions, the global growth of the transportation sector is undeniable, in both developing and developed countries, as the worldwide passenger travel vs. GDP by region in the figure below for the period 1950-1997 shows *[IPIECA Workshop, Baltimore, USA, 12-13 October 2004]*.


Figure 3: Passenger travel and GDP by region, 1950–97
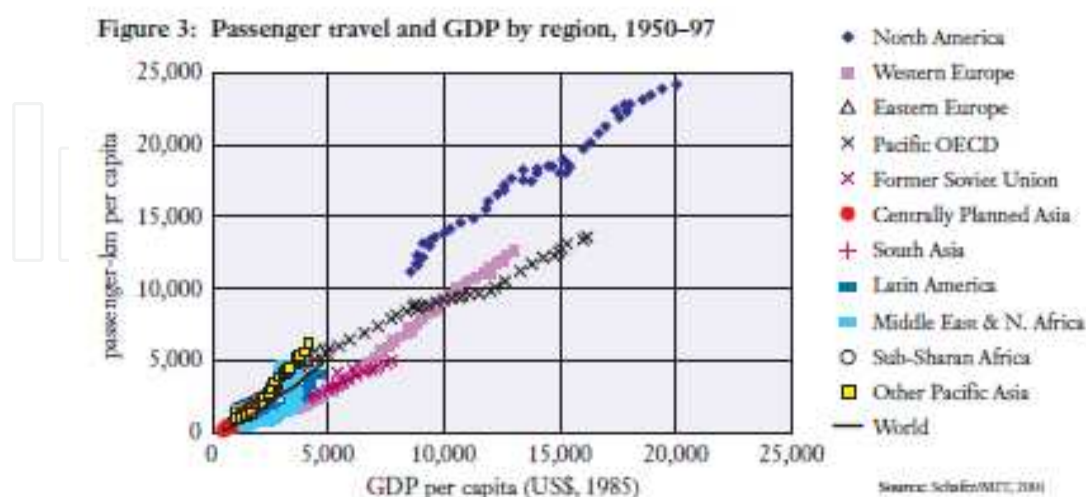
IPIECA Workshop, Baltimore, USA, 12-13 October 2004

In the EU, sectoral CO_2 emissions in 2005 for Energy, Transport, Industry, and Households were 34%, 27%, 21%, and 11%. The Transportation sector breakdown was Road (71.2%), Sea
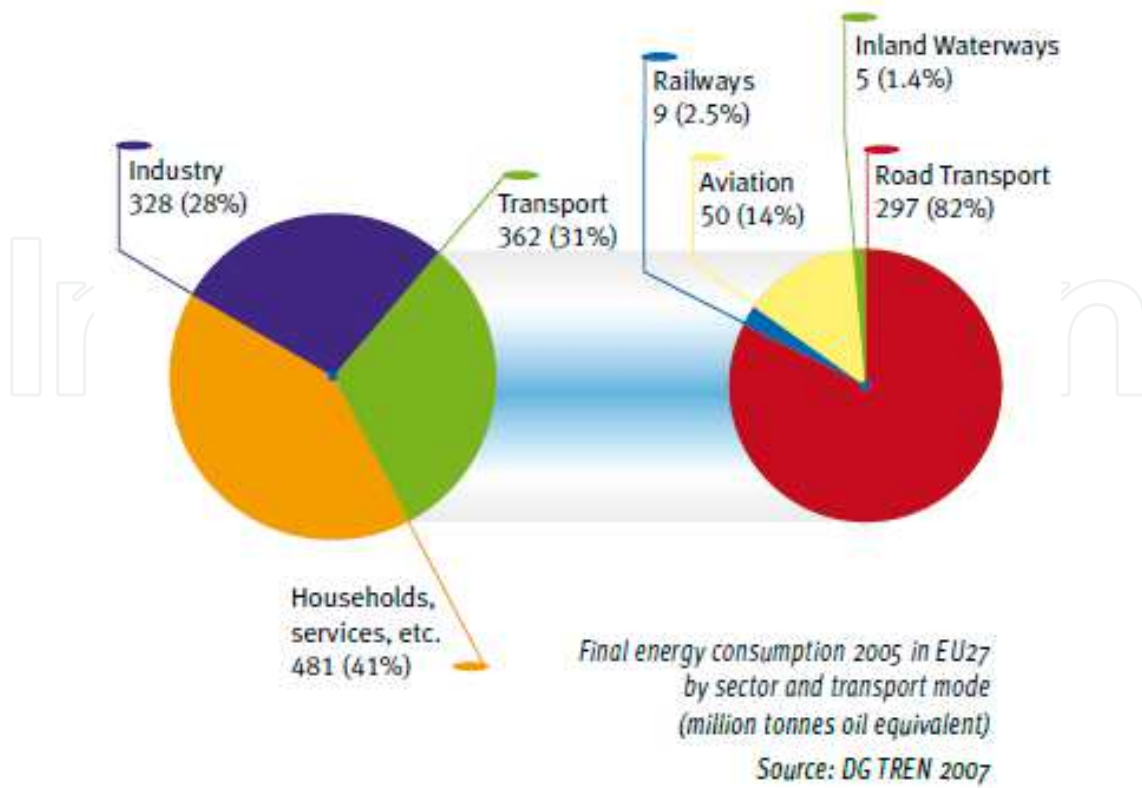
Industry
328 (28%)

Transport
362 (31%)

Railways
9 (2.5%)

Aviation
50 (14%)

Inland Waterways
5 (1.4%)

Road Transport
297 (82%)

Households,
services, etc.
481 (41%)

*Final energy consumption 2005 in EU27
by sector and transport mode
(million tonnes oil equivalent)*
Source: DG TREN 2007

From: Rail Transport and Environment, page 5 – Facts & Figures, Nov. 2008.

Local air pollution
(1 person, Berlin - Frankfurt, 545 km)

Source: www.ecopassenger.org 2008
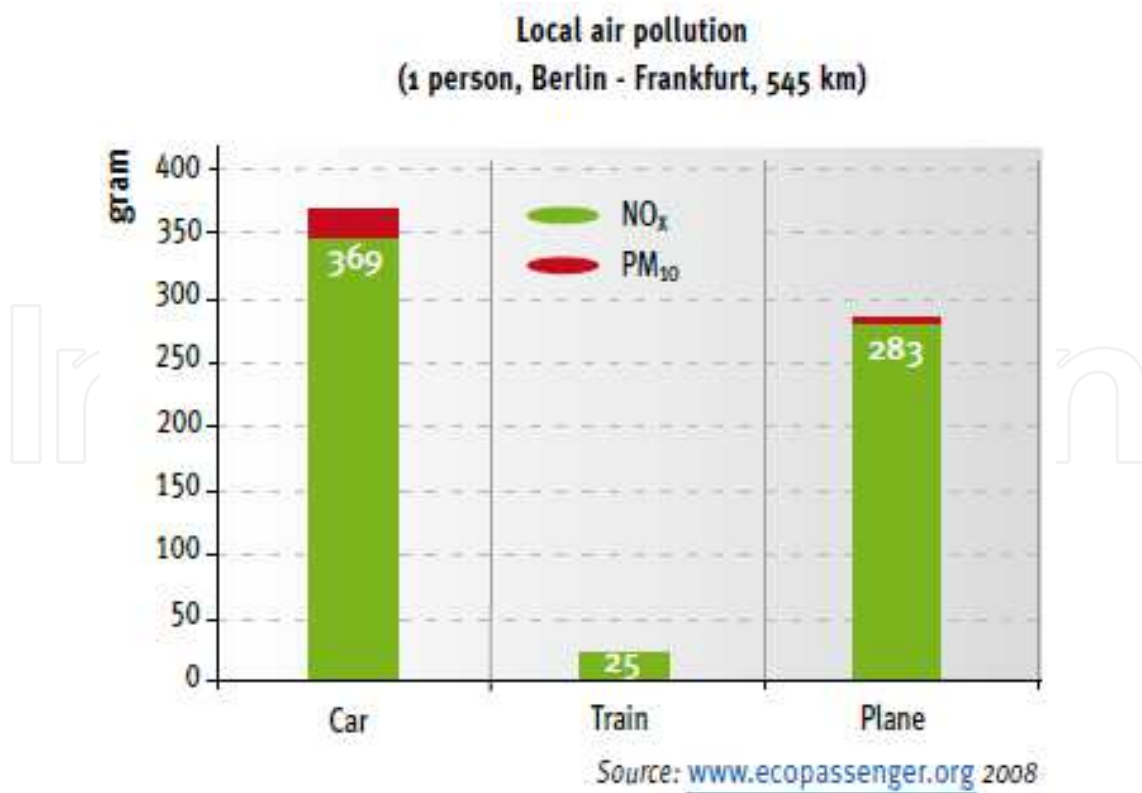
From: Rail Transport and Environment, page 20 – Facts & Figures, Nov. 2008

and Inland Waterways (14.5%), Aviation (11.9%). From: Rail Transport and Environment, page 5 – Facts & Figures, Nov. 2008 *[Rail Transport and Environment, page 5 – Facts & Figures, Nov. 2008]*. The sectoral energy consumption for 2005 appears in the figure shown below, from which the Transportation sector had the second largest share of 31% after the Households & Services sector. Aviation's share of the Transportation sector energy consumption was 14%, second to Road Transport. A similar trend would be found in other regions of the developed world which accounts for the bulk of the global energy consumption and carbon emission.

Similarly, local air pollution data for NO_x and PM_{10} appears below for a journey of 545 km by three modes of transportation.

Transportation of 100 tons of cargo for a distance of 700 km between the Netherlands and Switzerland generates the local pollution information as shown in the figure below:

Freight transport NO$_x$ and PM$_{10}$ comparison

The table below compares the local air pollution from transporting 100 tons of average goods from the port of Rotterdam, Netherlands, to Basel, Switzerland.

Local air pollution
(100 tons cargo, Basel - Rotterdam, 700 km)
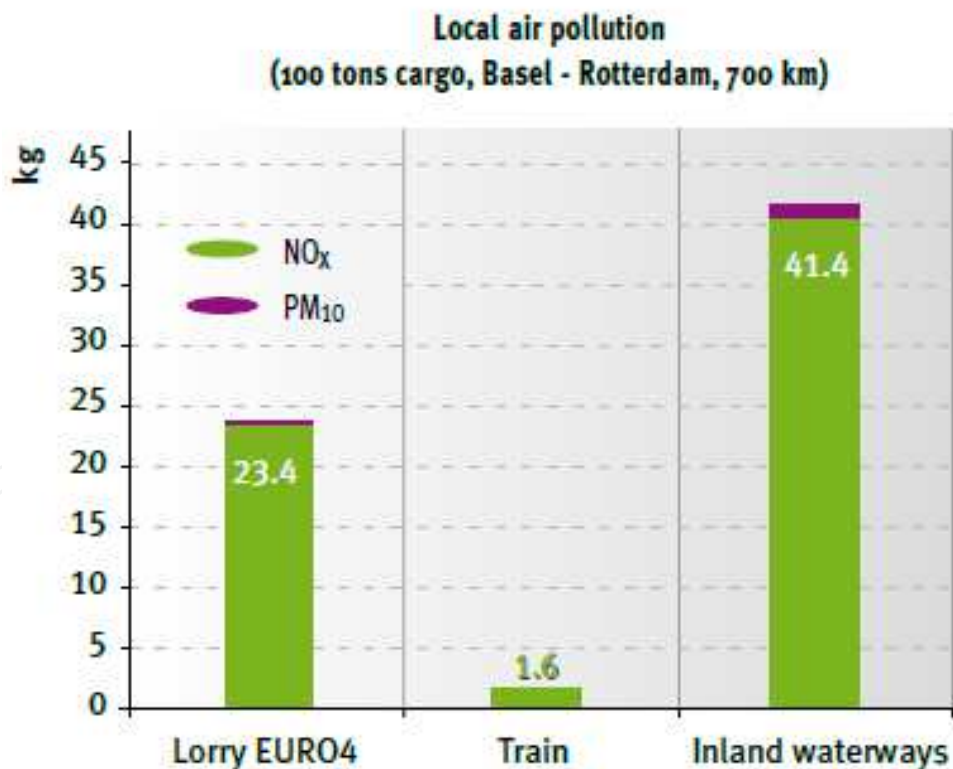
Source: www.ecotransit.org 2008

From: Rail Transport and Environment, page 19 – Facts & Figures, Nov. 2008.

Energy efficiency is of utmost importance in addressing the climate problem. Some significant strides have been made by some sub-sectors as the figure below indicates.

In Germany, the consumption of specific energy for Deutsche Bahn,
both for regional passenger trains and freight has decreased constantly
since 1990, due to the energy efficiency action plan of the company.

**Specific primary energy consumption (per pkm or tkm) 1990 - 2007,
Deutsche Bahn**
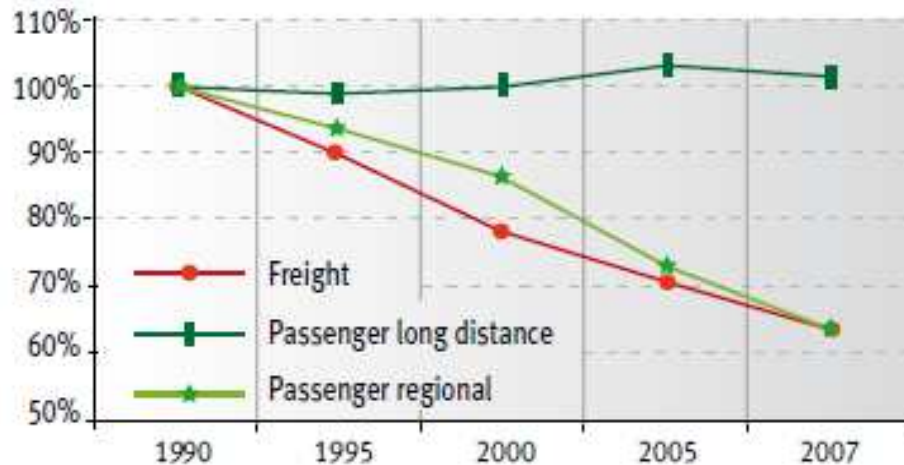
Source: Deutsche Bahn

From: Rail Transport and Environment, page 11 – Facts & Figures, Nov. 2008.

Finally, a look at the noise profile of some modes of transportation is instructive.

**Percentages of citizens who are "highly disturbed"
when exposed to rail, air and road traffic noise**
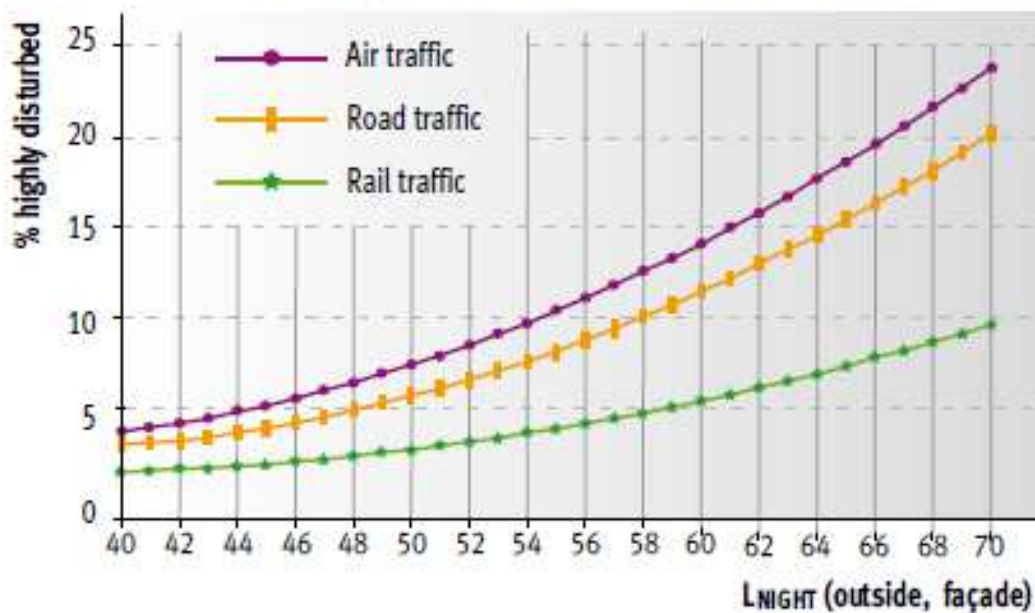
Source: EC 2004

From: Rail Transport and Environment, page 22 – Facts & Figures, Nov. 2008.

From the above, it is clear that just as the other sectors are called upon to reduce their GHG emission, the same should hold for the transportation sector. Gas turbines are employed in the air transportation sub-sector as well as in industry generally. It is claimed that air transport accounts for some 2-3 per cent of all anthropogenic CO2 emissions *[IPIECA Workshop, Baltimore, USA, 12-13 October 2004]*. As of 2004 IPIECA Workshop, there was no substitute envisioned for jet fuel neither was there any niche alternative fuel on the horizon. However, between 2008 and 2010, several test flights have been undertaken with synthetic jet fuel derived from natural gas *[Airline Industry Information, May 3, 2010]* as well as second generation biofuels from 50:50 blend of jathropha oil and standard A1 jet fuel *[The Seattle Times, Dec. 31, 2008]*. Similarly, the Airline Industry Information publication of 16 January 2009 reported that the US Federal Aviation Administration (FAA) has announced the results of a commercial airline test flight using a mixture of jet fuel and biofuel derived from algae and jatropha plants early in January 2009. In June 2009, the aviation fuels subcommittee of the ASTM International was reported to have approved specifications for synthetic aviation fuel, derived from a 50/50 blend of synthetic Fischer-Tropsch fuels and petroleum-derived fuels.

Gas turbines are employed in the Energy, Industrial, and the Transportation Sectors; sectors which have been shown to be responsible for most of the carbon emissions globally. Hence it is imperative to sustain the current drive for improvement in the energy, exergy and environmental performance of gas turbines in general (land, aviation, and marine gas turbine technology). We shall consider some of these issues in this chapter.

2. The Brayton open-cycle components – simple cycle and combined cycle gas turbines

Combustion Chamber/Combustor

Compressed air from the compressor (either centrifugal or axial-flow type) flows directly into the combustion chamber (such as that shown in Fig. 2.1 below) in a Brayton open simple cycle gas turbine where part of it (< 1/3) is used in a direct-fired air heater to burn the fuel after which the remaining air is mixed with the combustion products, all of which is to be carried out with minimum pressure loss. Minimization of pressure is critical at all stages from inlet to the compressor to entry into the turbine to ensure optimal power production from the gas turbine.

The Turbine Chamber of a 3-stage gas turbine plant is shown in Fig. 2.2 and Fig. 2.3 shows a typical turbine stage blades. Substantial volumes of air and combustion gases are moved smoothly and vibration-free through the gas turbine at very high velocities in an axial flow machine, being taken through a series of processes. These processes follow the Brayton cycle processes, viz.: non-isentropic compression from the atmospheric inlet conditions of the compressor to the isobaric (constant-pressure) combustion of the fuel in the combustion chamber, and then followed by adiabatic (non-isentropic) expansion of the hot gases and finally discharging the gases into the atmosphere, all of which is done in a continuous flow process. The energy transfer between the fluid and the rotor in the compression and expansion processes is achieved by means of kinetic action rather than by positive displacement as occurs as in reciprocating machines.

Fig. 2.1. A Combustion Chamber Can. [From Shepherd, D.G., Introduction to the Gas Turbine, D. Van Nostrand Co., Inc.
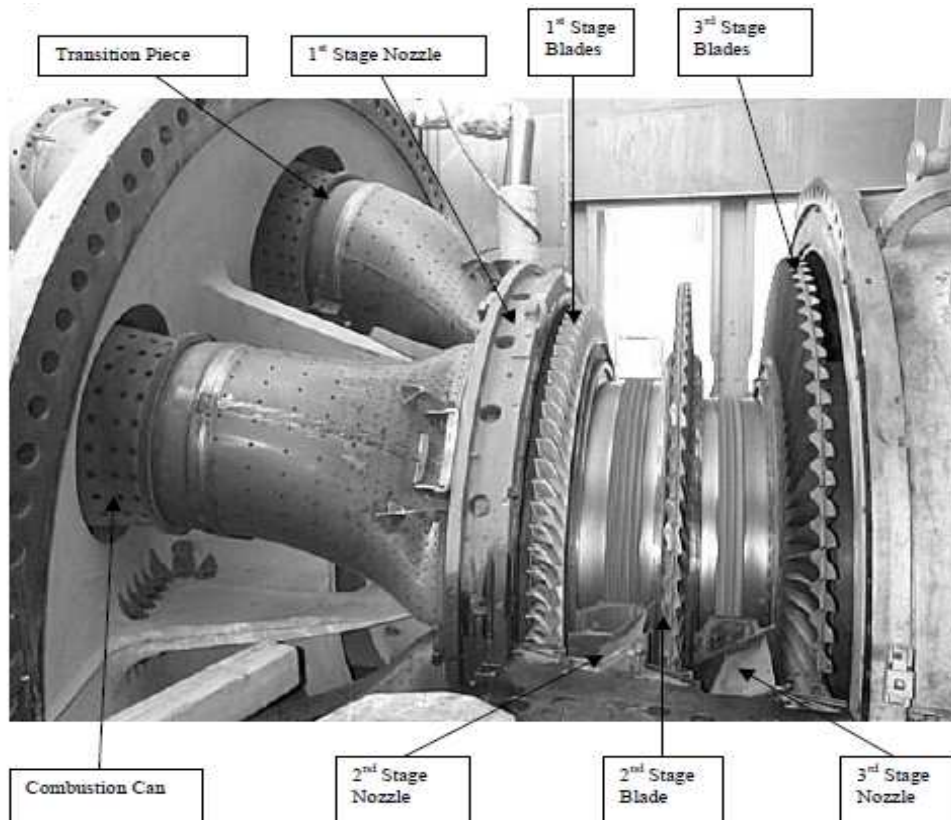

Fig. 2.2. The Turbine Chamber of a 3-stage turbine plant. [From Shepherd, D.G., Introduction to the Gas Turbine, D. Van Nostrand Co., Inc.

Fig. 3.3. Typical turbine stage. [From Shepherd, D.G., Introduction to the Gas Turbine, D. Van Nostrand Co., Inc.

4. Gas turbine fuels – conventional and new fuels

Conventional gas turbine fuels currently in use are exclusively liquid and gaseous and usually hydrocarbons. Solid gas turbine fuel technology is still in the research and developmental stages. New gas turbine fuels, as mentioned earlier in the Introduction, include the synthetic Fischer-Tropsch aviation jet fuels and the second generation biofuels.

Conventional gas turbine fuels – Liquid and gaseous fuels

Conventional gas turbine liquid fuels include the range of refined petroleum oils from highly refined gasoline through kerosene and light diesel oil to a heavy residual oil (Bunker C or No. 6 fuel oil). Table 4-1 gives the ultimate analysis of some liquid fuels.

Fuel	Carbon	Hydrogen	Sulfur	Ash, etc.
100 Octane petrol	85.1	14.9	0.01	-
Motor petrol	85.5	14.4	0.1	-
Benzole	91.7	8.0	0.3	-
Kerosene (paraffin)	86.3	13.6	0.1	-
Diesel oil	86.3	12.8	0.9	-
Light fuel oil	86.2	12.4	1.4	-
Heavy fuel oil	86.1	11.8	2.1	-
Residual fuel oil	88.3	9.5	1.2	1.0

Table 4.1. Ultimate analysis of some liquid fuels. (From Applied Thermodynamics for Engineering Technologists, S.I. Units by Eastop & McConkey, 2nd ed., 1970).

Table 4-2 below also indicates some of the key properties of some of the many known hydrocarbons.

Table 4.2. Abstracted from Table V Properties of Hydrocarbons of Steam, Air & Gas Power by Severns, Degler & Miles, John Wiley, 5th ed. 1964. S.I. Units conversion done by Prof. Richard Fagbenle. SIT – Self-ignition temperature;

Team, Air, and Gas Power Family Name	Formula	Melting Temp., °C	Boiling Temp., °C	SIT++ °C	Specific Gravity	API Gravity	HHV kJ/kg	LHV kJ/kg	Mixture kJ/m³
1. Gas C_nH_{2n+2} Methane	CH_4	-182.2	-161.1	730	0.424	202.5	55,475	50,235	3241.5
2. Gas C_nH_{2n+2} Ethane	C_2H_6	-172.2	-88.3	566	0.546	194.0	52,102	47,909	3439.0
3. LPG C_nH_{2n+2n} Propane	C_3H_8	-186.7	-42.2	535	0.582	142.0	50,358	46,555	3491.2
4. LPG C_nH_{2n+2n} Butane	C_4H_{10}	-135	-0.56	516	0.570	116.5	49,544	46,043	3532.1
5. LPG C_nH_{2n+2n} Pentane	C_5H_{12}	-129.4	36.1	501	0.626	94.5	49,079	45,583	3550.8
6. Gasoline C_nH_{2n+2n} n-Heptane	C_7H_{16}	-90.6	98.9	478	0.684	75.5	48,497	45,143	3591.8
7. Gasoline C_nH_{2n+2n} Triptane	C_7H_{16}	-25	81.1	……	0.690	……..	………	44,427	………
8. Gasoline C_nH_{2n+2n} Iso-Octane	C_8H_{18}	-107.8	99.4	732	0.692	73.5	47,869	44,564	3558.2
9. Fuel Oil C_nH_{2n+2} Decane	$C_{10}H_{22}$	-30	173.9	463	0.730	62.5	47,916	44,671	3599.2
10. Fuel Oil C_nH_{2n+2n} Dodecane	$C_{12}H_{26}$	-10	216.1	……	0.749	57.5	47,799	44,596	3610.4
11. Fuel Oil C_nH_{2n+2n} Hexadecane	$C_{16}H_{34}$	18.3	280	……	0.774	51.5	47,497	44,348	3610.4
12. Fuel Oil C_nH_{2n+2n} Octadecane	$C_{18}H_{38}$	27.8	307.8	……	0.782	49.5	47,450	44,303	3625.3
13. Olefins C_nH_{2n} Propene	C_3H_6	-185	-47.8	……	0.61	103.0	48,846	45,241	3595.5
14. Olefins C_nH_{2n} Butene-1	C_4H_8	-195	-6.7	……	0.625	……	48,613	45,008	3614.1
15. Olefins C_nH_{2n} Hexene-1	C_6H_{12}	-137.8	63.3	……	0.675	76.0	44,310	41,317	3576.9
16. Napthenes C_nH_{2n} Cyclopentane	C_5H_{10}	-94.4	49.4	……	0.746	56.7	43,682	40,691	3506.1
17. Naphthenes C_nH_{2n} Cyclohexane	C_6H_{12}	6.7	80.6	……	0.778	51.6	43,519	40,547	3506.1
18. Aromatics C_nH_{2n-6} Benzene	C_6H_6	5.6	80.6	739	0.88	29.0	42,240	39,984	3606.7
19. Aromatics C_nH_{2n-6} Toluene	C_7H_8	-95	110.6	811	0.87	31.0	42,566	40,612	3688.6
20. Aromatics C_nH_{2n-6} Xylene	C_8H_{10}	-26.1	140.6	……	0.86	31.0	43,031	40,705	3632.7
21. Alcohols Methanol	CH_3OH	-97.8	65	……	0.792	46.4	22,725	20,106	3353.3
22. Alcohols Ethanol	C_2H_6O	-117.2	77.8	……	0.785	47.1	29,726	26,991	3494.9
23. Tetraethyl lead	$C_8H_{20}Pb$	-136.1	182.2	……	1.653	……	………	…………	………
24. Hydrogen (gas)	H_2	………	……	……	……	……	………	10,002	………
25. Water	H_2O	0	100	……	0.998	……	………	0	………
26. Carbon (solid)	C	………	……	……	……	……	………	32,564	………
27. Gasoline (straight run)	……..	-60	43-149	……	……	……	………	44,194	………
28. Carbon monoxide	CO	………	-191.7	609	……	……	10,111	10,111	………

Fig. 4-1 below shows typical distillation characteristics for military and commercial aircraft fuels. Relative to the "pure substance" single evaporation temperatures of water and ethyl alcohol, gasoline is a mixture of liquid several hydrocarbons and its various components boil off at different temperatures as can be seen in the graphs.
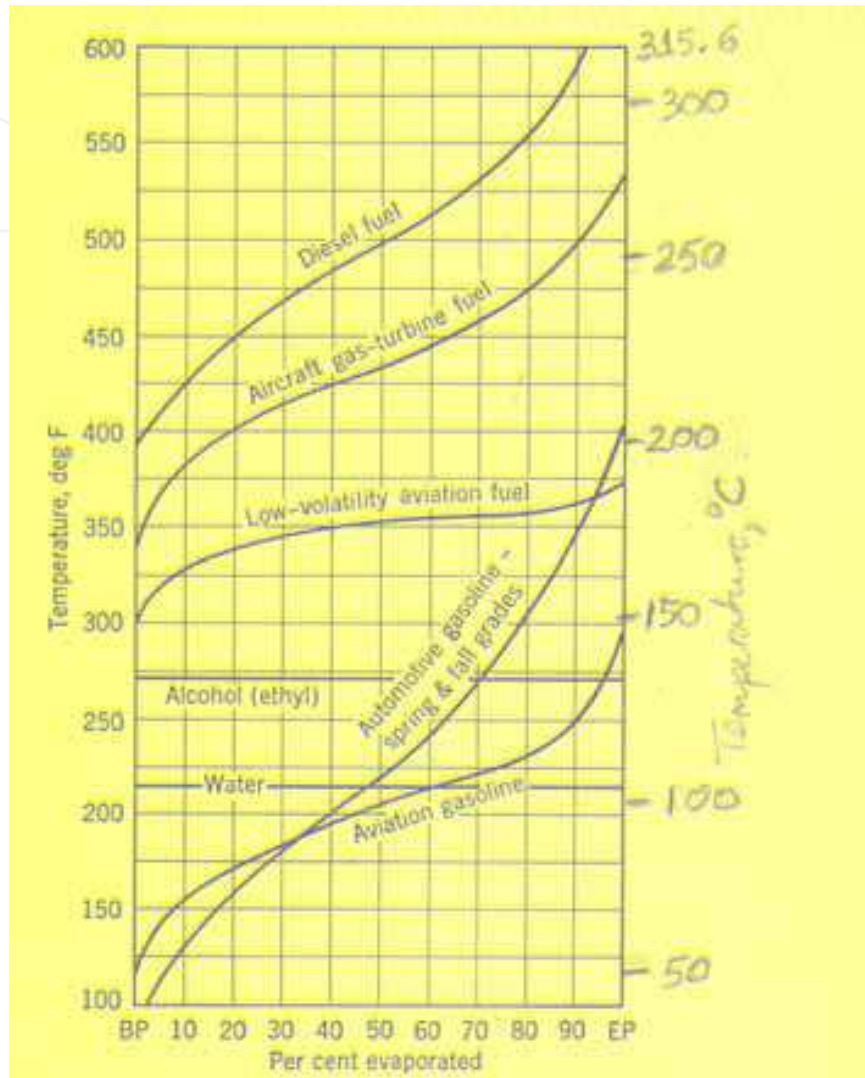

Fig. 4.1. Typical ASTM distillation characteristics for various types of fuels. Degree Centigrade scale supplied by Prof. R. 'Layi Fagbenle. Abstracted from Steam, Air, and Gas Power by Severns, Degler & Miles, John Wiley & Sons Inc. 1964.

The aviation gasoline graph at the bottom of the graph is for piston-engine powered aircraft and it has a low flash point to improve its ignition characteristics. It is usually a high-octane gasoline known as "avgas". Turbine engines on the other hand can operate with a wide range of fuels, but typically use fuels with much higher flash points, less flammable and generally safer to store and transport. Most jet fuels are basically kerosene-based. Both the Jet A specification fuel used in the USA and the Jet A-1 standard specification of most of the rest of the world have a relatively high flash point of 38°C and a self-ignition temperature (SIT) (or auto-ignition temperature) of 210°C, making them safer to handle than the traditional avgas. The open air burning temperature in Table 4-2 can be compared with the typical distillation characteristics for aircraft gas turbine fuel in Fig. 4-1.

Physical Properties	Jet A-1	Jet A
Flash Point	> 38°C (100.4 °F)	
Self- (auto-) ignition temperature	210 °C (410 °F)	
Freezing point	< -47 °C (-52.6 °F)	< -40 °C (-40 °F)
Open air burning temperature	287.5 °C (549.5 °F)	
Density (per litre)	0.775 kg/l – 0.840 kg/l	
Specific energy (calorific value)	> 42.80 MJ/kg	

Table 4.2. Typical Specifications for Jet A and Jet A-1 Aircraft Fuels (from Wikipedia)

Specifications for Heavy-Duty Gas Turbine Fuels

Heavy-duty gas turbines are able to burn a wide range of gaseous fuels and hence are less restricted in their fuel classifications. A typical heavy-duty gas turbine fuel specification (range only indicated) appears in Table 4-3 below.

Fuel	LHV [MJ/m^3]	Major Components
Natural Gas and Liquefied Natural Gas (LNG)	29.81 – 7.45	Methane
Liquefied Petroleum Gas [LPG]	85.70 – 119.23	Propane; Butane
Gasification Gases (Air Blown)	3.73 – 5.50	CO; H_2; N; H_2O_v
Gasification Gases (Oxygen Blown)	7.45 – 14.90	CO; H_2; H_2O_v
Process Gases	11.20 – 37.30	CH_4; H_2; CO; CO_2

Table 4.3. Range of typical heavy-duty gas turbine fuel classification (adapted from GEI 41040G – GE Gas Power Systems, Revised January 2002).

The feedstock for gasification fuels can be coal, petroleum coke or heavy liquids. Gasification fuels generally have lower much lower heating values than other fuel gases, and they are produced by one of two processes: oxygen blown or air blown gasification process.

Process gases are generated by many petrochemical and chemical processes and are suitable for fuelling gas turbines, for example refinery gases). Constituents of process gases include CH_4, H_2, CO, and CO_2. Other process gases used as gas turbine fuels are byproducts of steel production such as blast furnace gases and coke oven gases. Blast Furnace Gases (BFG) have heating values below minimal allowable limits for gas turbine fuels, necessitating blending with other fuels such as coke oven gas, natural gas or hydrocarbons such as propane or butane.

Typical gas turbine fuel specification ranges appear in Table 4-4 below. In addition to such specifications which may be particular to each turbine manufacturer, allowable gas fuel contaminant levels are also specified for such trace metals as (Pb, V, Ca, and Mg), Alkali metals (Na and K) and particulates. Sodium (Na) is the only trace metal contaminant normally found in natural gas, and it source is salt water in the ground gas wells.

Sources of contaminants in heavy-duty gas turbine applications include particulates arising largely from corrosion chemical reactions in gas pipelines, liquid (water and/or hydrocarbon) condensates and lubricating oils from compressor stations; sulfur (as H_2S or COS); trace metals; steam and water for injection; alkali metals contained in compressor discharge; and the fuel.

Fuel Properties	Max	Min	Notes
Lower Heating Value, MJ/m^3	None	3.73 –11.20	

Modified Wobbe Index (MWI)
  - Absolute limits
  - Range within limits
	54
	+5%
		40
		-5%	

Flammability Ratio		2.2:1	Rich:Lean Fuel/Air Ratio, volume basis
Constituent Limits, mole % Methane, CH_4	100	85	% of reactant species
Ethane, C_2H_6	15	0	% of reactant species
Propane, C_3H_8	15	0	% of reactant species
Butane C_4H_{10} + higher paraffins (C_4+)	5	0	% of reactant species
	Trace	0	% of reactant species
Hydrogen, H_2	Trace	0	% of reactant species
Carbon monoxide, CO	Trace	0	% of reactant species
Oxygen, O_2	Trace	0	% of reactant species
Total Inerts (N_2+CO_2+Ar)	15	0	% of total (reactants + inerts)
Aromatics (Benzene C_6H_6, Toluene C_7H_8, etc.)	Report	0	
Sulfur	Report	0	

Table 4.4. Range of typical heavy-duty gas turbine fuel specification (adapted from GER 41040G – GE Gas Power Systems, Revised January 2002).

Conventional and New Environmental-conscious Aero and Industrial Gas Turbine Fuels

Conventional aero gas turbine fuels are commonly:
i. Kerosene from crude petroleum sources using established refining processes, and
ii. synthetic kerosene from Fischer-Tropsch (FT) synthesis using coal, natural gas, or any other hydrocarbon feedstock (e.g. shale, tar sands, etc.). These are produced by first gasifying the hydrocarbon resource followed by liquefaction to form hydrocarbon liquids (e.g. as earlier noted, the Airline Industry Information update dateline 26 June 2009)

New Environmentally-conscious aero gas turbine fuels are:
i. Bio-fuels from bio-derived Fatty Acid Methyl Esters (FAME) mixed with conventional aero fuel (kerosene) in regulated proportions,
ii. Bio-ethanol and bio-methanol neat or mixed in regulated proportions with gasoline,
iii. Biofuels produced from Fischer-Tropsch Synthesis (FTS) process using biomass feedstock such as oil seeds – jathropha, palm oil, soybeans, rapeseed (canola), sunflower, camelina, etc., as well as animal fats,
iv. Bio-syngas produced by gasification of biomass, lignocellulosic biomass and other agricultural wastes used as feed into the FTS (2nd generation biofuels) to produce liquid fuels (FTL), and
v. Liquefied petroleum gas (LPG) which is really not a cryogen; Liquefied gases such as LNG, Methane and Hydrogen. Both methane and hydrogen will have to be liquefied for use as aircraft fuel.

Table 4.5 below gives relative properties of conventional aviation kerosene and typical biodiesel aircraft fuel (will vary with Fatty Acid Methyl Esters [FAME] type):

Property	Aviation Kerosene	Bio-diesel	20% Blend	Impact
Heat of combustion [MJ/kg] typical	43.2	32 – 39	41.0 – 42.4 (spec. min: 42.8)	Airframe range/loading
Density [kg/m^3] range	775 – 840	860 – 900	792 – 852	
Viscosity [mm2/sec @ -20°C max.				Wing tank temp. limits, Cold Starts & Relight.
Approx. Carbon length	C14 – C15 max (trace levels)	C16 – C22	C16 – C22	Combustion emissions
Flash point, °C min.	38	>101	Unchanged	
Freeze Point,°C max	-47	-3? 0	-5 to -10 with additives	Wing tank temp. limits, Cold Start and Relight.
Sulfur [ppm] max	3000	10		
Acidity [mg KOH/g] max	0.015	0.5	0.11	Material compatibility
Phosphorous [ppm] max	Excluded	10	2	Hot-end life
Metals [ppm] max	Excluded	5	1	Hot-end life
Thermal Stability	Controlled to well defined level	Not controlled	Not known	Fuel system & injector life
Composition	Hydrocarbon	FAME	20% FAME	Elastomer compatibility

From: Ppt. Presentation by Chris Lewis, Company Specialist – Fluids, Rolls Royce plc, titled "A Gas Turbine Manufacturer's View of Biofuels". 2006.

In the steam-reforming reaction, steam reacts with feedstock (hydrocarbons, biomass, municipal organic waste, waste oil, sewage sludge, paper mill sludge, black liquor, refuse-derived fuel, agricultural biomass wastes and lignocellulosic plants) to produce bio-syngas. It is a gas rich in carbon monoxide and hydrogen with typical composition shown in Table 4.6 below.

Constituents	% by vol. (dry & N$_2$-free)
Carbon monoxide (CO)	28 – 36
Hydrogen (H$_2$)	22 – 32
Carbon dioxide (CO$_2$)	21 – 30
Methane (CH$_4$)	8 – 11
Ethene (C$_2$H$_4$)	2 – 4
Benzene-Toluene-Xylene (BTX)	0.84 – 0.96
Ethane (C$_2$H$_5$)	0.16 – 0.22
Tar	0.15 – 0.24
Others (NH3, H2S, HCl, dust, ash, etc.)	< 0.021

Source: M. Balat et al. Energy Conversion and Management 50 (2009) 3158 – 3168).

Table 4.6. Typical composition of bio-syngas from biomass gasification.

A useful reference for the thermo-conversion of biomass into fuels and chemicals can be found in the above referenced paper by M. Balat et al.

Ethanol-powered gas turbines for electricity generation

In a 2008 report by Xavier Navarro (RSS feed), a company called LPP Combustion (Lean, Premixed, Prevaporized) was claimed to have demonstrated that during gas turbine testing, emissions of NOx, CO, SO_2 and PM (soot) from biofuel ethanol (ASTM D-4806) were the same as natural gas-level emissions achieved using dry low emission (DLE) gas turbine technology. It was also claimed that the combustion of the bio-derived ethanol produced virtually no net CO_2 emissions.

Gas Turbines and Biodiesels

A recent study by Bolszo and McDonnell (2009)[1] on emissions optimization of a biodiesel-fired 30-kW gas turbine indicates that biodiesel fluid properties result in inferior atomization and longer evaporation times compared to hydrocarbon diesel. It was found that the minimum NOx emission levels achieved for biodiesel exceeded the minimum attained for diesel, and that optimizing the fuel injection process will improve the biodiesel NOx emissions.

A theoretical study was recently carried out by Glaude et al. (2009)[2] to clarify the NOx index of biodiesels in gas turbines taking conventional petroleum gasoils and natural gas as reference fuels. The adiabatic flame temperature T_f was considered as the major determinant of NOx emissions in gas turbines and used as a criterion for NOx emission. The study was necessitated by the conflicting results from a lab test on a microturbine and two recent gas turbine field tests, one carried out in Europe on rapeseed methyl ester (RME) and the other in USA on soybean methyl ester (SME), the lab test showing a higher NOx emission while the two field tests showed slightly lower NOx emission relative to petroleum diesel. It is however clear that biodiesels have reduced carbon-containing emissions and there is agreement also on experimental data from diesel engines which indicate a slight increase in NOx relative to petroleum diesel. The five FAME's studied by Glaude et al. were RME, SME, and methyl esters from sunflower, palm and tallow.

The results showed that petroleum diesel fuels tend to generate the highest temperatures while natural gas has the lowest, with biodiesel lying in-between. This ranking thus agrees with the two field tests mentioned earlier. It was also found out that the variability of the composition of petroleum diesel fuels can substantially affect the adiabatic flame temperature, while biofuels are less sensitive to composition variations.

5. Factors limiting gas turbine performance

The Joule cycle (also popularly known as the Brayton cycle) is the ideal gas turbine cycle against which the performance (i.e. the thermal efficiency of the cycle η_{CY}) of an actual gas turbine cycle is judged under comparable conditions. We prefer to restrict the use of Joule

---

[1] C. D. Bolszo and V. G. McDonell, Emissions optimization of a biodiesel fired gas turbine, Proceedings of the Combustion Institute, Vol 32, Issue 2, 2009, Pages 2949-2956.

[2] Pierre A. Glaude, Rene Fournet, Roda Bounaceur and Michel Moliere, (2009). Gas Turbines and Biodiesel: A clarification of the relative NOx indices of FAME, Gasoil and Natural Gas.

cycle to the ideal gas turbine cycle while the Brayton cycle is exclusively used for the actual gas turbine cycle. The ideal gas turbine "closed"cycle (or Joule cycle) consists of four ideal processes – two isentropic and two isobaric processes – which appear as shown in Fig. 5.1. The thermal efficiency of the Joule cycle in terms of the pressure ratio r_p given by $r_p = \frac{p_B}{p_A}$ and the pressure ratio parameter ρ_p given by $\rho_p = r_p^{(\gamma-1)/\gamma}$ is:

$$\eta_{\text{Joule}} = \left(1 - \frac{1}{r_p^{(\gamma-1)/\gamma}}\right) = \left(1 - \frac{1}{\rho_p}\right) \tag{5.1}$$

Hence, the thermal efficiency of the ideal gas Joule cycle is a function only of the pressure ratio. Since for isentropic processes 1-2 and 3-4, $\frac{T_2}{T_1} = \frac{T_3}{T_4} = \rho_p$, the Joule efficiency is also dependent of the isentropic temperature ratios only, but independent of the compressor and the turbine inlet temperatures separately without a knowledge of the pressure ratio. Thus, ρ_p is essentially the isentropic temperature ratio, the abscissa in Fig. 5.1. If air is the working fluid employed in the ideal Joule cycle, the cycle is referred to as the air-standard Joule cycle.
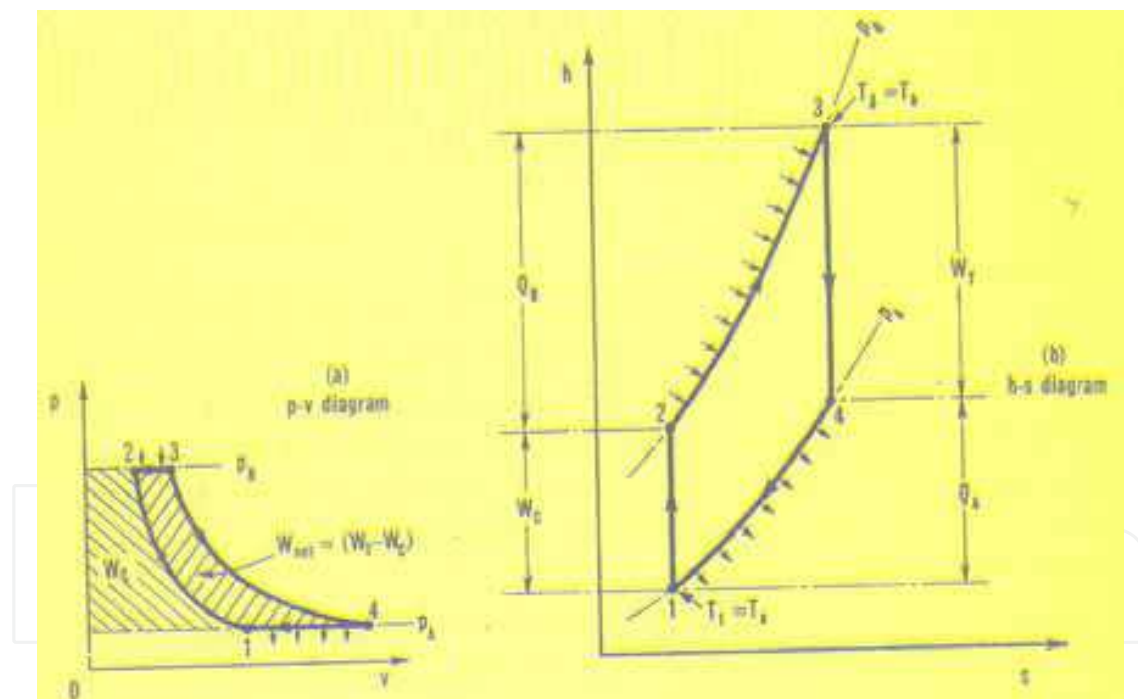
Fig. 5.1. Ideal Joule cycle (a) p-V and (b) T-s state diagrams. From Haywood [ ].

Fixing the inlet temperature to the compressor T_a and the inlet temperature to the turbine T_b automatically sets a limit to the pressure ratio r_p, which occurs when the temperature after isentropic compression from T_a is equal to the TIT T_b. However, when this occurs, the net work done is seen to be equal to zero, as the area of the cycle on the T-s and p-V diagrams indicate.

Haywood considers an interesting graphical representation of eq. 5.1 above for $T_a = 15°C$ and $T_b = 100°C$ as shown in Fig. 5.2

Fig. 5.2. Variation of cycle efficiency with Isentropic temperature ratio ρ_p (t_a = 15°C). From Haywood [ ].
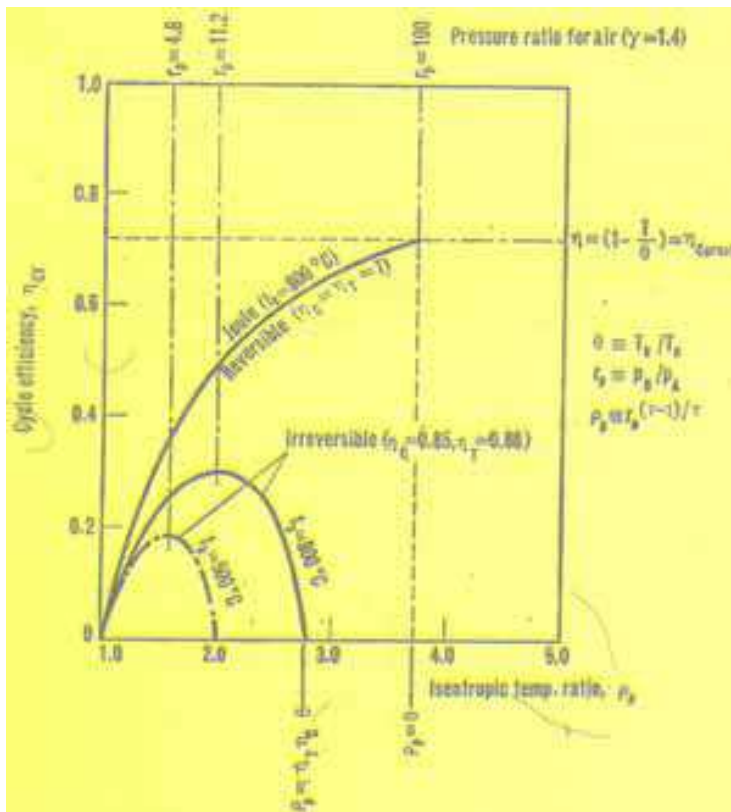
For T_a = 15°C and T_b = 100°C, η_{Joule} increases continuously with rp right up to the limiting value as the curve labeled "reversible" shows. The limiting pressure ratio r_p = 99.82 approximated to 100 in the figure is attained when $\rho_p = \theta = T_b/T_a = 1073/288 = 3.7257$. Under this condition, a sketch of the Joule cycle on the T-s diagram shows that as r_p approaches this value, the area enclosed by the cycle approaches zero. However, In practical terms, a pressure ratio this large is never used when issues of process irreversiblities are considered, to which the remaining two curves in the graph pertain.

5.1 Effect of irreversibilities in the actual gas turbine cycle

In an actual plant, frictional effects in turbines and compressors and pressure drops in heat exchangers and ductings and combustion chamber are basically lost opportunities for production of useful work. The h-s curve diagram for such a gas turbine Brayton cycle appears in Fig. 5.3, wherein the heat and work terms in each of the processes are identified, ignoring the frictional effects in the heat exchangers, ductings and combustion chamber. We note that the compressor work input required W_C, is now much larger than its previous value for the ideal Joule cycle while the turbine work output W_T is considerably smaller than for the ideal Joule cycle, revealing the considerable effect of turbine and compressor inefficiencies on the cycle thermal efficiency. An analytic expression for the Brayton cycle thermal efficiency can be shown to be:

$$\eta_{Brayton} = \frac{(1-1/\rho_p)(\alpha-\rho_p)}{(\beta-\rho_p)} \qquad (5.2)$$

where $\alpha = \eta_C\eta_T\theta$, $\beta = [1 + \eta_C(\theta-1)]$, and $\theta = T_b/T_a$.

In Fig. 5.2, the actual Brayton cycle performance is depicted for turbine and compressor isentropic efficiencies of 88% and 85% respectively, t_a = 15°C for two values of t_b = 800°C and 500°C respectively. The optimum pressure ratio is now reduced from approximately 100 to 11.2 for t_b = 800°C, and to only 4.8 at t_b = 500°C. This optimum pressure ratio is more realistically achievable in a single compressor. Here also, we find that $\eta_{Brayton}$ is highly dependent on $\theta = T_b/T_a$, showing a drastic reduction from TIT = 800°C to TIT = 500°C.
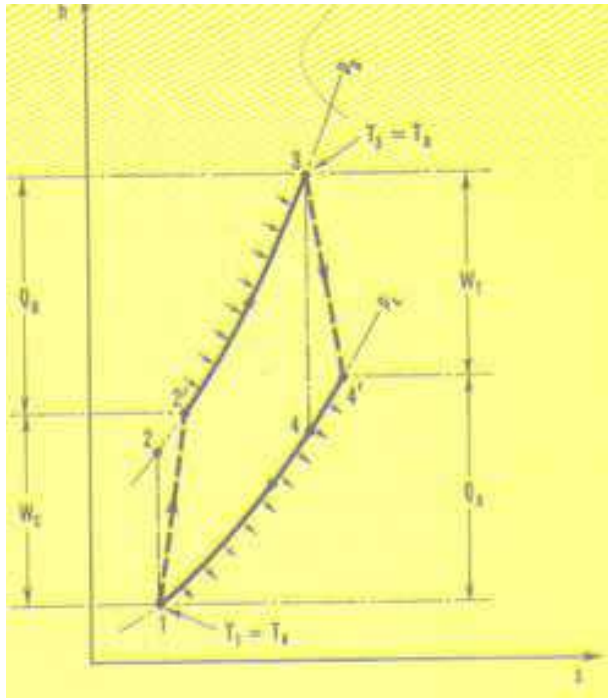
The compressor work input per unit mass of working fluid is

$$W_c = c_p(T_{2'} - T_a) = \frac{c_p T_a}{\eta_c}(\rho_p - 1) \qquad (5.3)$$

while

$$W_T = c_p(T_b - T'_4) = c_p \eta_T T_b \left(1 - \frac{1}{\rho_p}\right) \quad (5.4)$$

and

$$W_{net} = (W_T - W_C) = \frac{c_p T_a}{\eta_c}\left(1 - \frac{1}{\rho_p}\right)(\alpha - \rho_p) \quad (5.5)$$

with $\alpha = \eta_C \eta_T \theta$ and $\theta = T_b/T_a$ as before.

From 5.5, W_{net} vanishes when $\rho_p = 1$ and when $\rho_p = \alpha$. Also from differentiating 5.5 w.r.t. ρ_p, we obtain that W_{net} is maximum when $\rho_p = \sqrt{\alpha}$. The variation of W_{net} with the adiabatic temperature ratio ρ_p appears in Fig. 5.4.

Fig. 5.3. Enthalpy-entropy diagram for Actual Brayton cycle, with turbine and Compressor inefficiencies. From Haywood [ ].
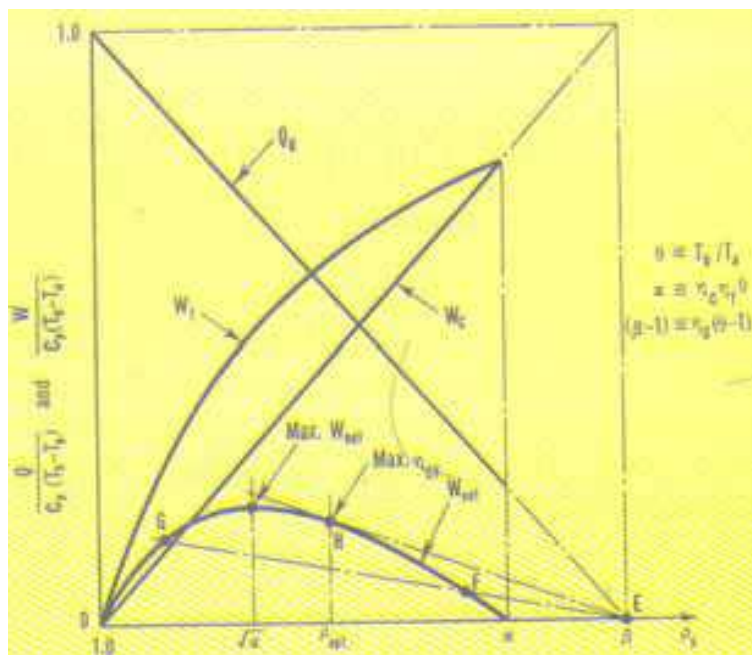
Haywood [] discusses the graphical construction in Fig. 5.4 due to Hawthorne and Davis [ ] for the variation of Q_B, W_T, W_C, and W_{net} with variation in ρ_p for fixed values of T_a and T_b. The maximum efficiency is obtained at the value of ρ_p corresponding to the point H at which a straight line from point E is tangent to the curve for W_{net}, i.e at $\rho_p = \rho_{opt}$. The method indicates that the points of maximum thermal efficiency of the Brayton cycle η_{CY} and the maximum W_{net} are not coincident; rather the value of ρ_p is greater for the former than for the latter. It may also be shown that, if ρ_W and ρ_{opt} are the values of ρ_p for maximum W_{net} and maximum η_{CY} respectively, then $\frac{\rho_w}{\rho_{opt}} = \sqrt{(1 - \eta_m)}$ where η_m is the maximum value of the thermal efficiency of the Brayton cycle.

Fig. 5.4. Variation of heat supplied to the combustor Q_B, turbine work output W_T, compressor work input W_C, and W_{net} with isentropic temperature ratio ρ_p. From Haywood [ ].

Figs. 5.5 and 5.6 show the schematic of the simple-cycle, open-flow gas turbine with a single shaft and double shaft respectively. The single shaft units are typically used in applications requiring relatively uniform speed such as generator drives while in the dual shaft applications, the power turbine rotor is mechanically separate from the high-pressure turbine and compressor rotor. It is thus aerodynamically coupled, making it suitable for variable speeds applications.
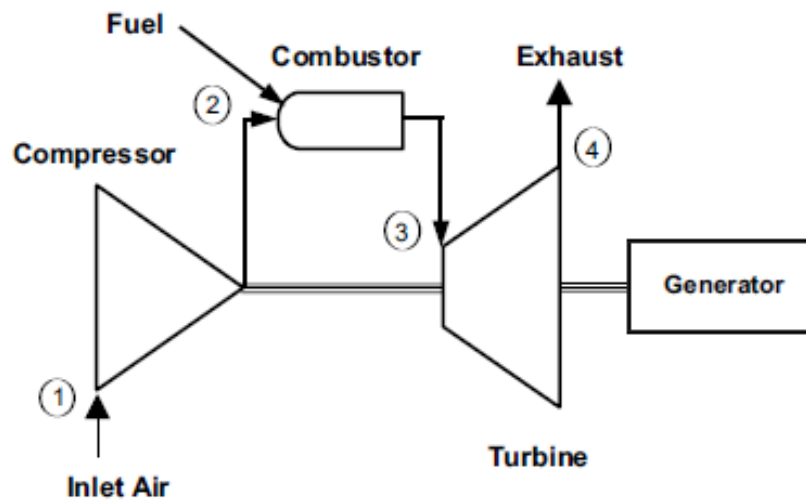

Fig. 5.5. Simple-cycle, open-flow, single-shaft gas turbine
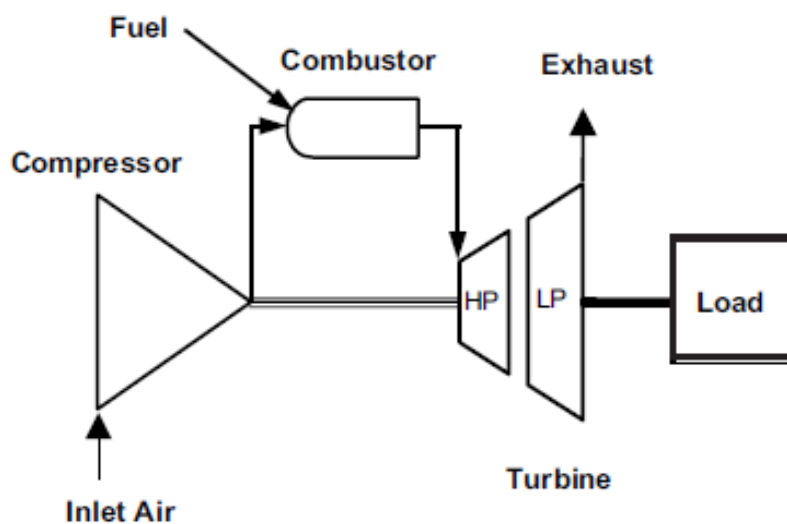
Fig. 5.6. Simple cycle, open-flow, dual-shaft gas turbine for mechanical drives.

5.2 Simple-cycle vs. Combined-cycle gas turbine power plant characteristics

Fig. 5.7 shows the variation of output per unit mass and efficiency for different firing temperatures and pressure ratios for both simple-cycle and combined-cycle applications. In the simple-cycle top figure, at a given firing temperature, an increase in pressure ratio results in significant gains in thermal efficiency. The pressure ratio resulting in maximum efficiency and maximum output are a function of the firing temperature; the higher the pressure ratio, the greater the benefits from increased firing temperature. At a given

pressure ratio, increasing the firing temperature results in increased power output, although this is achieved with a loss in efficiency mainly due to increase in cooling air losses for air-cooled nozzle blades.

On the other hand, pressure ratio increases do not affect efficiency markedly as in simple-cycle plants; indeed, pressure ratio increases are accompanied by decreases in specific power output. Increases in firing temperature result in marked increases in thermal efficiency. While simple-cycle efficiency is readily achieved with high pressure ratios, combined-cycle efficiency is obtained with a combination of modest pressure ratios and higher firing temperatures. A typical combined-cycle gas turbine as shown in Fig. 5.7 (lower cycle) will convert 30% to 40% of the fuel input into shaft output and up to 98% of the remainder goes into exhaust heat which is recovered in the Heat Recovery Steam Generator (HRSG). The HRSG is basically a heat exchanger which provides steam for the steam turbine part of the combined-cycle. It is not unusual to utilize more than 80% of the fuel input in a combined-cycle power plant which also produces process steam for on- or off-site purposes.
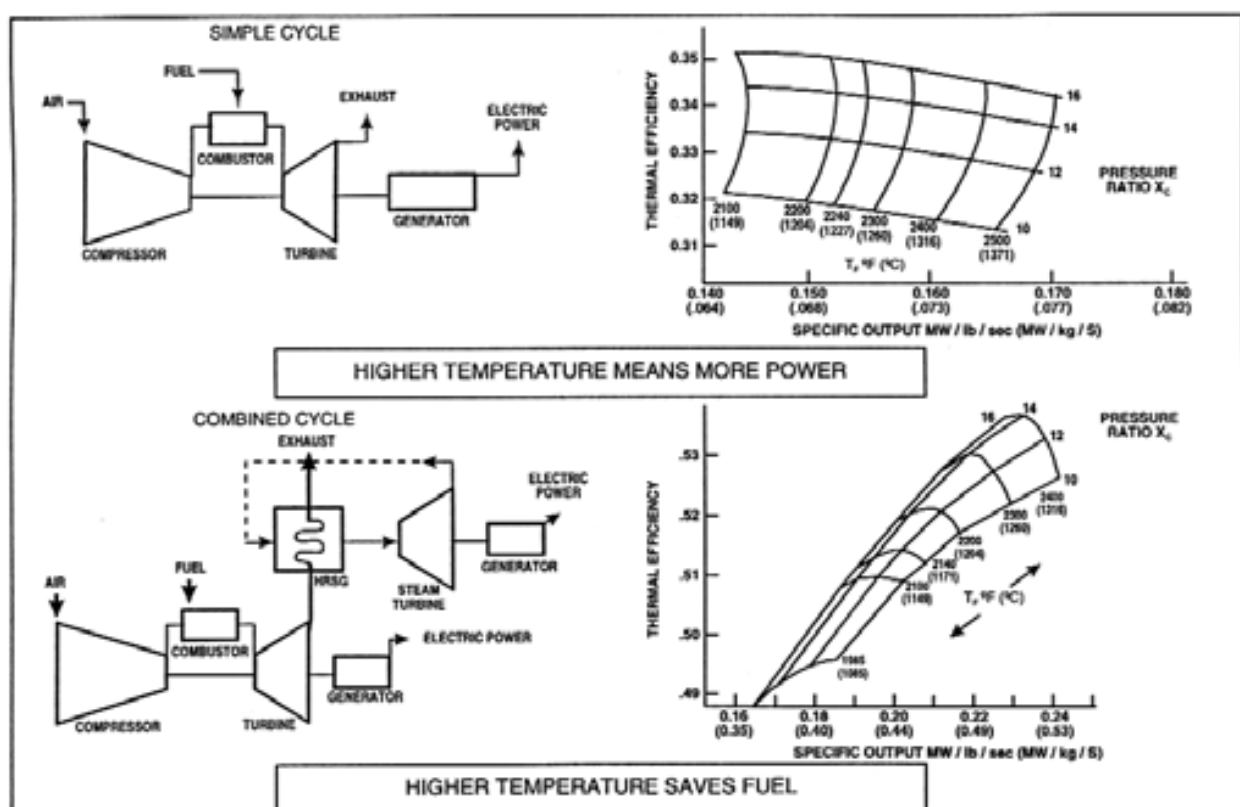

Fig. 5.7. Gas turbine characteristics for simple-cycle (above) and for combined-cycle (below). Abstracted from GE Power Systems.GER-3567H 10/00.

5.3 Other factors affecting gas turbine performance

Other factors affecting the performance of a gas turbine (heat rate, power output) include the following: Air temperature (compressor inlet temperature) and pressure; Site elevation or altitude; humidity; inlet and exhaust losses resulting from equipment add-ons such as air filters, evaporative coolers, silencers, etc. The usual reference conditions stated by manufacturers are 59F/15C and 14.7 psia/1.013 bar. In general, output decreases with increasing air temperature while the heat rate increases less steeply. Similarly, altitude

corrections are provided by manufacturers with factors less than 1.0 at higher latitudes. The density of humid air is less than that of dry air and it affects both the heat rate and the specific output of a gas turbine. The higher the humidity, the lower the power output and conversely the higher the heat rate. Inlet and exhaust pressure losses result in power output loss, heat rate increase and exhaust temperature increase.

5.4 Gas turbine emissions and control

Over the past three to four decades, many developed countries have put in place applicable state and federal environmental regulations to control emissions from aero, industrial and marine gas turbines. This was the case even before the current global awareness to the Climate Change problem. Only NOx gas turbine emission was initially regulated in the early 1970s and it was found that injection of water or steam into the combustion zone of the combustor liner did produce the then required low levels of NOx reduction without serious detrimental effects on the gas turbine parts lives or the overall gas turbine cycle performance. However, as more stringent requirements emerged with time, further increase in water/steam approach began to have significant detrimental effects on the gas turbine parts lives and cycle performance, as well increased levels of other emissions besides NOx. Alternative or complimentary methods of emission controls have therefore been sought, some internal to, and others external to, the gas turbine, namely:

i.   Dry Low NOx Emission (DLN) or DLE burner technology
ii.   Exhaust catalytic combustion technology
iii. Overspray fogging

While NOx emissions normally include Nitrous oxide (NO) and Nitrogen dioxide (NO_2), NOx from gas turbines is predominantly NO, although NO_2 is generally used as the mass reference for reporting NOx. This can be seen from the typical exhaust emissions from a stationary industrial gas turbine appearing in Table 5.1.

Major Species	Typical Concentration (% Volume)	Source
Nitrogen (N_2)	66 - 72	Inlet Air
Oxygen (O_2)	12 - 18	Inlet Air
Carbon Dioxide (CO_2)	1 - 5	Oxidation of Fuel Carbon
Water Vapor (H_2O)	1 - 5	Oxidation of Fuel Hydrogen
Minor Species Pollutants	**Typical Concentration (PPMV)**	**Source**
Nitric Oxide (NO)	20 - 220	Oxidation of Atmosphere Nitrogen
Nitrogen Dioxide (NO_2)	2 - 20	Oxidation of Fuel-Bound Organic Nitrogen
Carbon Monoxide (CO)	5 - 330	Incomplete Oxidation of Fuel Carbon
Sulfur Dioxide (SO_2)	Trace - 100	Oxidation of Fuel-Bound Organic Sulfur
Sulfur Trioxide (SO_3)	Trace - 4	Oxidation of Fuel-Bound Organic Sulfur
Unburned Hydrocarbons (UHC)	5 - 300	Incomplete Oxidation of Fuel or Intermediates
Particulate Matter Smoke	Trace - 25	Inlet Ingestion, Fuel Ash, Hot-Gas-Path
		Attrition, Incomplete Oxidation of Fuel or
		Intermediates

Table 5.1. Typical exhaust emissions from a stationary industrial gas turbine. Abstracted from GE Power Systems – GER-4211-03/01.

NOx are divided into two main classes depending on their mechanism of formation. NOx formed from the oxidation of free nitrogen in either the combustion air of the fuel are known as "thermal NOx", and they are basically a function of the stoichiometric adiabatic flame temperature of the fuel. Emissions arising from oxidation of organically bound nitrogen in the fuel (the fuel-bound-nitrogen, FBN) are known as "organic NOx". Of the two, efficiency of conversion of FBN to NOx proceeds much more efficiently than that of thermal NOx.
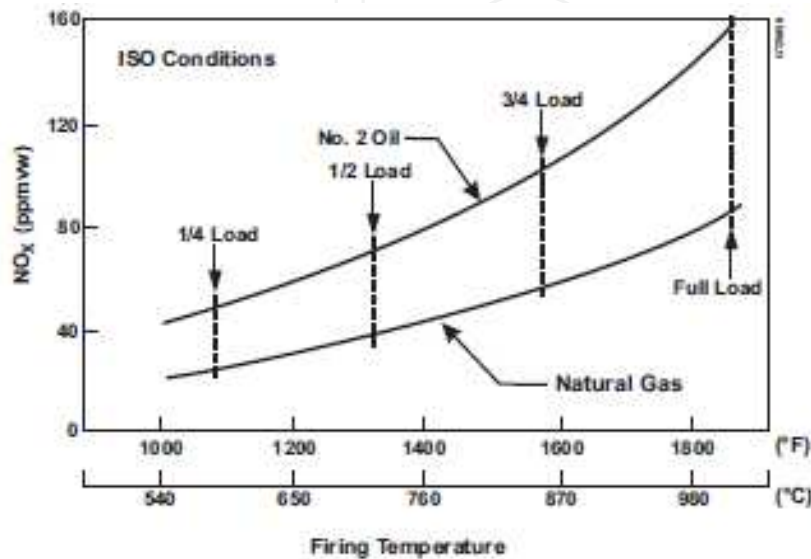
Fig. 5.8. Typical NOx emissions for a class of Industrial gas turbines. Abstracted from GE Power Systems – GER-4311-03/01.
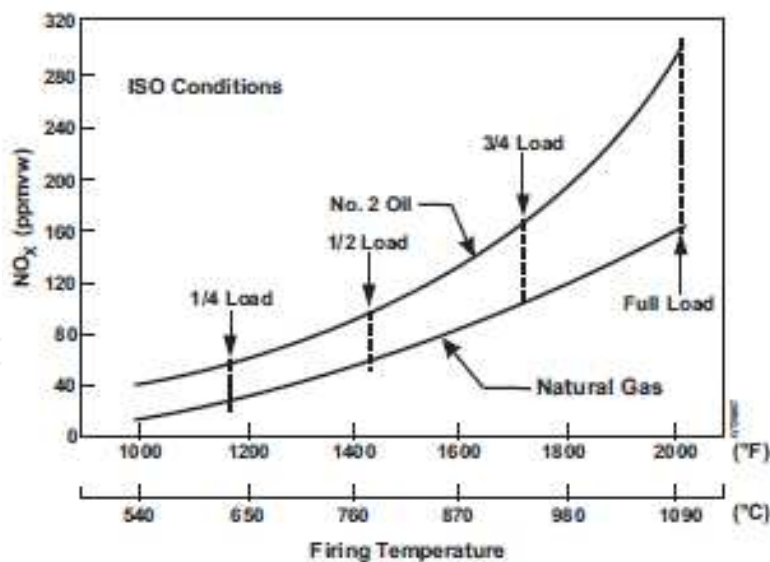
Fig. 5.9. Typical NOx emissions for a class of Industrial gas turbines. Abstracted from GE Power Systems – GER-4311-03/01.

Thermal NOx is relatively well studied and understood, but much less so for organic NOx formation. For thermal NOx production, NOx increases exponentially with combustor inlet air temperature, increases quite strongly with F/A ratio or with firing temperature, and increases with increasing residence time in the flame zone. It however decreases exponentially with increasing water or steam injection or increasing specific humidity. Figs.

5.1 and 5.2 show typical NOx emissions for industrial gas turbines operating on natural gas fuel and No.2 distillate as a function of firing temperature.

As regards organic NOx, reduction of flame temperature (as through water or steam injection) does scant little to abate it. Water and steam injection are known to actually increase organic NOx in liquid fuels. As noted earlier, organic NOx is important only for fuels containing significant amount of FBN such as crude or residual oils.

Carbon Monoxide (CO) emissions as seen from Table 5.1 can be of comparable magnitude with NO emission, depending on the fuel and the loading condition of the gas turbine. Fig. 5.10 is a typical industrial gas turbine CO emission as a function of firing temperature. We note that, contrary to the NOx trend, CO emission increases significantly as the firing temperature is reduced below about 816°C (1500°F). It is noted that carbon monoxide is normally expected from incomplete combustion and hence inefficiency in the combustion process.
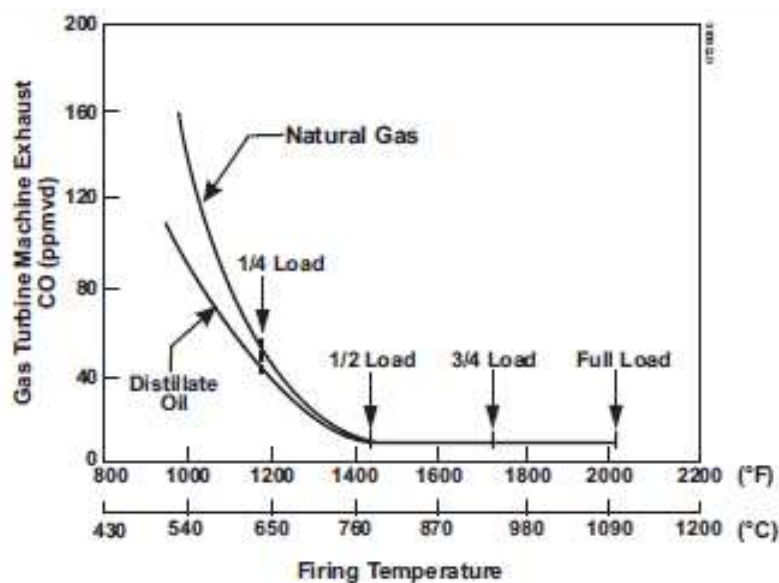

Fig. 5.10. CO emissions from an industrial gas turbine. Abstracted from GE Power Systems – GER-4311-03/01.
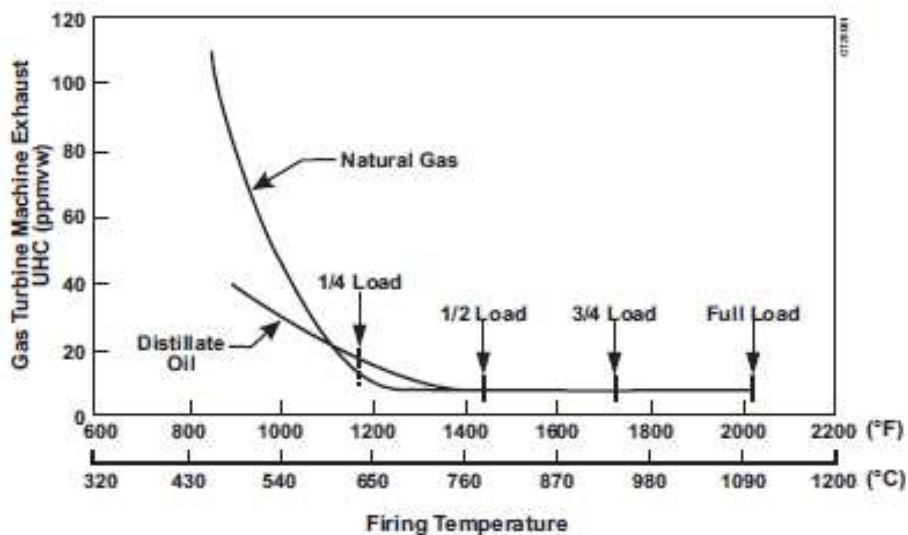

Fig. 5.11. UHC emissions from an industrial gas turbine. Abstracted from GE Power Systems – GER-4311-03/01.

Unburned hydrocarbons (UHC) are also products of the inefficiency in the combustion process. Fig. 5.11 shows a typical industrial gas turbine UHC emission as a function of firing temperature.

Particulates.

Fuel properties, combustor operating conditions and the design of the combustor all affect the gas turbine exhaust particulate emission, whose main components are smoke, ash, erosion and corrosion products in the metallic ducting and piping of the system.

Gas Turbine Emission Control Techniques

Emission	Control technique
NOx	Lean Head End Liner; Water or Steam Injection; Dry Low NOx Emission (DLE); Overspray fogging
CO	Combustor Design; Catalytic reduction
UHC & VOC	Combustor Design
SOx	Control of sulfur in fuel
Particulates & PM-10	Fuel composition influencing Sulfur & Ash;
Smoke	Combustor design; Fuel composition; Air atomization

6. Exergy considerations

Publication of research articles on exergy consideration in power cycles dates back about four decades now, possibly with the initial work of Kalina (1984) on the combined cycle system with novel bottoming cycle and that of El-Sayed and Tribus (1985) on a theoretical comparison of the Rankine and Kalina cycles. This was followed with the work of Zheng et al. (1986a) on Energy Utilization Diagram (EUD) for two types of LNG power-generation systems; Zheng (1986b) on graphic exergy analysis for coal gasification-combined power cycle based on EUD; Ishida et al. (1987) on evaluation of a chemical-looping-combustion power-generation system by graphic exergy analysis; and Wall et al. (1989) ending the first decade with an exergy study of the Kalina cycle that began the decade.

In the second decade belong the works of Najjar (1990) on hydrogen fuelled and cooled gas turbines; Ishida et al. (1992a) on graphic exergy analysis of fuel-cell systems based on EUDs; Jin & Ishida (1993) on graphical analysis of complex cycles; Joshi et al. (1996) on a review of IGCC technology; and Jaber et al. (1998) on gaseous fuels (derived from oil shale) for heavy-duty gas turbines and Combined Cycle Gas Turbines.

The third decade began with the analysis of Bilgen (2000) on exergetic and engineering analysis of gas turbine-based cogeneration systems; Thongchai et al. (2001) on simplification of power cycles with EUDs; Marrero et al. (2002) on 2nd law analysis and optimization of a combined triple power cycle; Jin & Ishida (2004) on graphic presentation of exergy loss in mixing on an EUD; Khaliq (2004) on second-law analysis of the Brayton/Rankine combined power cycle with reheat; Khaliq (2004b) on thermodynamic performance evaluation of combustion gas turbine cogeneration systems with reheat; Ertesvag et al. (2005) on exergy analysis of a gas turbine combined cycle power plant with pre-combustion CO_2 capture; Tae won Song et al. (2006) on performance characteristics of a MW-class SOFC/GT hybrid system based on a commercially available gas turbine; Guillermo Ordorica-Garcia et al. (2006) on technoeconomic evaluation of IGCC power plants for CO_2 avoidance; Fagbenle et

al (2007) on thermodynamic analysis of biogas-fired integrated gasification steam-injected gas turbine (BIG/STIG) plant; Karellas et al. (2008) on thermodynamic evaluation of combined cycle plants; Fadok et al. (2008) on an update on advanced hydrogen turbine development; Bartieri et al. (2008) on biomass as an energy resource – the thermodynamic constraints on the performance of the conversion process in producing synthetic gas (syngas) for high efficiency internal combustion engines such as CCGT as well as in fuel cells (MCFC and SOFC) after adequate cleaning up and reforming; Khaliq (2009a) on exergy analysis of a gas turbine trigeneration system for combined production of power, heat and refrigeration; Khaliq (2009b) on energy and exergy analyses of compression inlet air-cooled gas turbines using the Joule-Brayton refrigeration cycle; Khaliq (2009c) on exergy analysis of the regenerative gas turbine cycle using absorption inlet cooling and evaporative aftercooling; Farzaneh-Gord et al. (2009) on a new approach for enhancing performance of a gas turbine using as a case study the Khangiran refinery in Iran; Fachina (2009) on Exergy accounting – the energy that matters; and finally closing the highly productive decade with Baratieri et al. (2009) on the use of syngas in IC engines and CCGT.

The fourth decade has begun with Woudstra et al. (2010) on thermodynamic evaluation of combined cycle plants. This does in no way claim to be a complete account of all the contributions to exergy analyses of power cycles from inception to the present time, rather we have tried to give some highlights on the journey so far.

Exergetic Analyses of Power Cycles – Gas Turbines, CCGTs, IGCC & BIG/STIG

Dincer and Rosen (2007) have listed the following benefits of using exergy analysis in industrial plant equipment and processes:

- Efficiencies based on exergy, unlike those based on energy, are always measures of the approach to true ideality, and therefore provide more meaningful information when assessing the performance of energy systems. Also, exergy losses clearly identify the locations, causes and sources of deviations from ideality in a system.
- In complex systems with multiple products (e.g., cogeneration and trigeneration plants), exergy methods can help evaluate the thermodynamic values of the product energy forms, even though they normally exhibit radically different characteristics.
- Exergy-based methods have evolved that can help in design-related activities. For example, some methods (e.g., exergoeconomics and thermoeconomics) can be used to improve economic evaluations. Other methods (e.g., environomics) can assist in environmental assessments.
- Exergy can improve understanding of terms like energy conservation and energy crisis, facilitating better responses to problems.

The following table comparing energy and exergy from Dincer & Cengel [ ] is also useful in appreciating exergy.

According to Szargut et al. [1988], "exergy is the amount of work obtainable when some matter is brought to a state of thermodynamic equilibrium with the common components of the natural surroundings by means of reversible processes, involving interaction only with the above mentioned components of nature". Four different types of exergy are identifiable in principle, denoted as kinetic, potential, physical and chemical exergy, Masim and Ayres [ ], viz.:

$$\varepsilon = \varepsilon_k + \varepsilon_p + \varepsilon_{ph} + \varepsilon_{ch}$$

ENERGY	EXERGY
Is dependent on the parameters of matter or energy flow only, and independent of the environment parameters.	Is dependent on both the parameters of matter or energy flow and on the environment parameters.
Has the values different from zero (equal to mc^2 upon Einstein's equation)	Is equal to zero (in dead state by equilibrium with the environment).
Is governed by the 1st Law of Thermodynamics (FLT) for all the processes.	Is governed by the 1st Law of Thermodynamics (FLT) for reversible processes only (while it is destroyed partly or completely in irreversible processes).
Is limited by the 2nd Law of Thermodynamics (SLT) for all processes (including reversible ones).	Is not limited for reversible processes due to the 2nd Law of Thermodynamics (SLT).
Is motion or ability to produce motion.	Is work or ability to produce work.
Is always conserved in a process, so can neither be destroyed or produced.	Is always conserved in a *reversible* process, but is always consumed in an irreversible process.
Is a measure of quantity only.	Is a measure of quantity and quality due to entropy.

Table 6.1.

Kinetic and potential exergy (ε_k & ε_p) have the same meaning as their corresponding energy or work terms, W_k and W_p, both of which are usually negligible in the analysis of most common industrial processes. Physical exergy is the work obtainable by taking a substance through reversible physical processes from its initial state at temperature T and pressure p to the final state determined by the temperature T_o and pressure p_o of the environment, Szargut et al. [1988]. Consideration of physical exergy is important for optimization of thermal and mechanical processes including heat engines and power plants. However, it is of secondary importance and often negligible when attention is focused on very large systems, such as chemical and metallurgical processes, where chemical exergy dominates in resource accounting and environmental analyses Masim and Ayres [ ]. Chemical exergy is the work that can be obtained by bringing a substance having the temperature and pressure (T,p) to a state of thermodynamic equilibrium with the datum level components of the environment. It has two components – one associated with chemical reactions occurring in isolation, and the other associated with the diffusion of reaction products into the surroundings, Masim and Ayres [ ]. Hence the importance of defining a reference state when calculating both physical and chemical exergy. The exergy function is thus a measure of the difference between two states, namely the state of the "target" system and that of its surroundings (or, more appropriately, the ultimate state of the combined system plus its surroundings, after they have reached mutual equilibrium of pressure p_o, temperature T_o, and chemical composition μ_o). As Masim and Ayres [ ] put it, the analytical expression for exergy shows that exergy is a measure of the "thermodynamic distance" of the target system from equilibrium, or alternatively, a measure of the "distinguishability" of the target system from its environment.

For a closed system with (T,p), the exergy (loss) $\Delta\varepsilon$ is given by:

$$\Delta\varepsilon = B = S(T - T_o) - V(p - p_o) + \sum \mu_i(N_i - N_{io})$$

where Ni is the number of moles of the ith system and μ_i is its chemical potential. As noted earlier, $\Delta\varepsilon \leq 0$, the equality holding only when the process is reversible. Here p_o and T_o are, appropriately, the ambient atmospheric pressure and temperature respectively.

For a flow or open system, where mass crosses the system boundaries,

$$\Delta\varepsilon = B = (H - H_o) - T_o(S-S_o) - \sum\mu_i(N_i - N_{io})$$

where H is enthalpy. In this case, it is important to have a knowledge of the detailed average chemical composition of the reaction products and the environmental sink with which the system reacts Masim and Ayres [ ].

Exergetic Analyses of Gas Turbine Cogeneration/Combined Cycle Plants

The generic name "*Cogeneration or Combined Cycle*" plants is used for gas turbine top cycle plant whose hot exhaust is used for generating steam in a heat recovery steam generator (HRSG) for a steam turbine bottom cycle. In these plants, the gas turbine combustion chamber (combustor) is fuelled normally with liquid or gaseous fuels piped to the plant from nearby storage tanks; the fuel is thus not produced on-site. Cogeneration/Combined Cycle plants therefore generate additional power from the steam turbine. However, they may also generate both power and steam from the steam turbine if process steam is required on-site or elsewhere, as in district heating systems. In such a case, the Cogeneration/CC plant would properly qualify to be called a Combined Heat and Power (CHP) Plant, although this appellation is technically reserved for any power plant whose hot combustion product gases are used to generate steam for on-site or other uses. Thus a CHP need not have a gas turbine in its power production train, it could be any power plant that generates "waste" heat from which we are able to extract "useful" thermal energy. In this regard, many CHP plants are powered by large diesel Internal Combustion (I.C.) engines.

We first consider the work of Bilgen (2000) on exergetic analyses of gas turbine cogeneration systems in which gas turbine cogeneration systems involving three different combinations of power and steam generation from a gas turbine and a steam turbine fed with steam from a HRSG were studied (see Figures 6.1, 6.2 and 6.3). The gas turbine exhaust gases produce the steam in the HRSG.
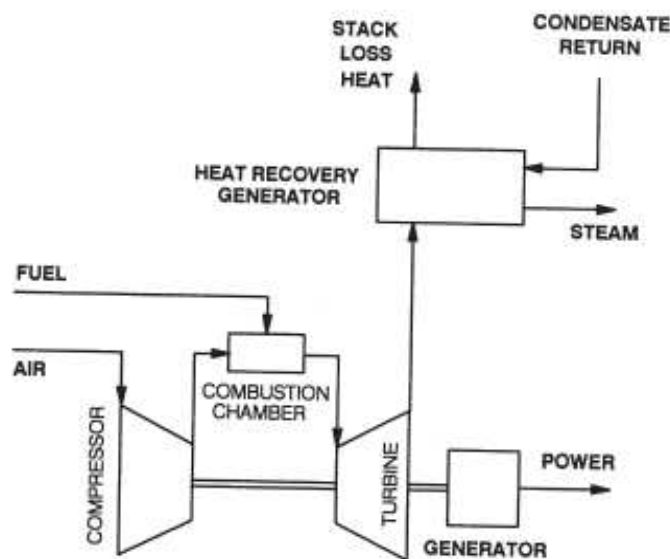
Schematic of the cycle for gas turbine electric power production–process heat production.

Fig. 6.1. From Bilgen (2000).
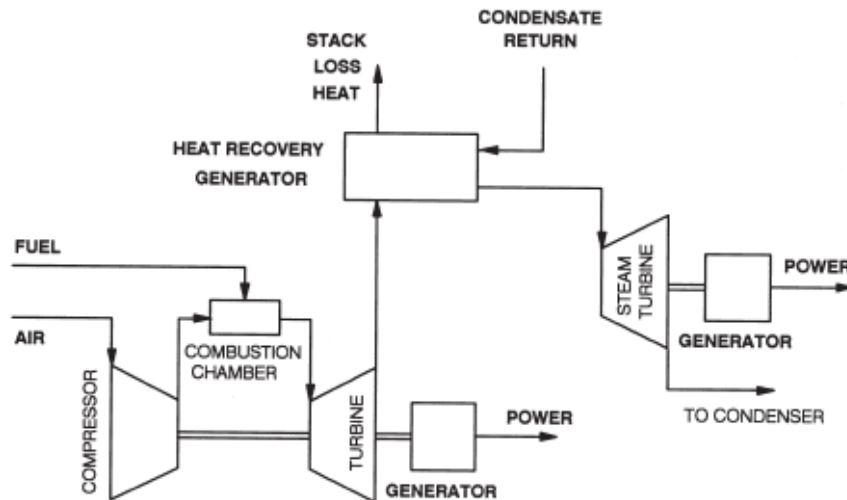
Schematic of the cycle for gas turbine electric power production–electric power production by steam turbine.
Fig. 6.2. From Bilgen (2000)
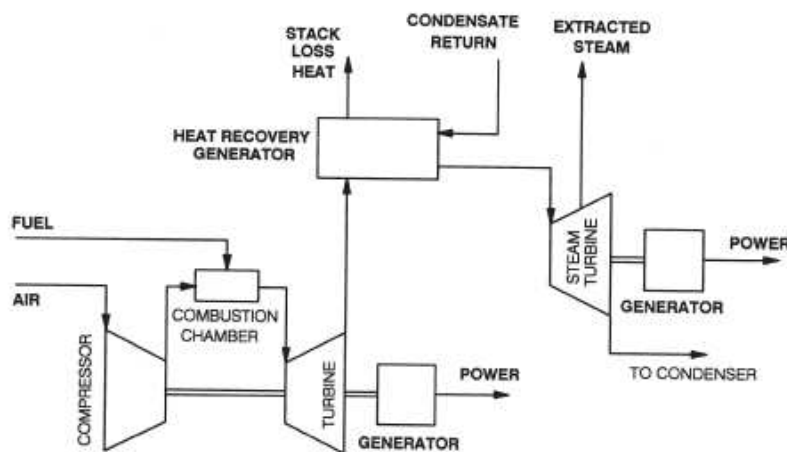
Fig. 3.   Schematic of the cycle for gas turbine electric power production–electric power production by steam turbine–
process heat production.

Fig. 6.3. From Bilgen (2000).

Bilgen undertook a combustion analysis by calculating the composition of the fuel gas mixture using direct minimization of the Gibbs function of formation of each compound I from its constituent elements, using Lagrangian multipliers. The fuel utilization efficiency or the 1st Law efficiency is given by

$$\eta = C\frac{(W_e + Q_p)}{E_f} \qquad (6.1)$$

Where E_f is the energy of the fuel, W_e and Q_p are the electrical energy and the thermal energy of the process respectively while C is 0.98 as the parasitic system loss is assumed to be 2%. The second law or exergy efficiency is defined as

$$\varepsilon = \frac{(W_e + B_p)}{B_f} \qquad (6.2)$$

Where We is work, hence considered all exergy as earlier discussed, Bp is the exergy content of process heat produced and Bf is the exergy content of fuel input. Expressions for the energy and exergy terms above were given by Bilgen as follows:

$$E_f = \sum_p n_e h_e - \sum_r n_i h_i \qquad (6.3)$$

$$B_f = \left(\sum_r n_i g_i - \sum_p n_e g_e\right) + RT_o \ln\left(\frac{y_{O_2}^{y^1}}{y_{CO_2}^{x^1} y_{H_2O}^{x^2}}\right) \qquad (6.4)$$

where h_i, h_e are enthalpies and g_i, g_e are the Gibbs functions of reactants (shown with r) and products (shown with p) for stoichiometric reaction of fuel evaluated at 1 bar and 298 K; y_i^α is the mole fraction of component I in the environment.

A fuel exergy factor is defined as

$$\varepsilon_f = \frac{B_f}{E_f} \qquad (6.5)$$

The exergy of the process heat produced is given by

$$B_p = m_s[(h-h_c) - T_o(s-s_c)] \qquad (6.6)$$

where m_s and s are the mass and entropy of the steam produced, sc is the entropy of the condensate return, both at the process heat pressure, and T_o is temperature of the environment. Further,

$$Q_p = m_s(h-h_c) \qquad (6.7)$$

Process heat exergy factor and power-to-heat ratio are defined as

$$\varepsilon_p = \frac{B_p}{Q_p} \qquad \text{and} \qquad r_{ph} = \frac{W_e}{Q_p} \qquad (6.8a,b)$$

A relationship can be established between exergy, ε, and fuel utilization, η, efficiencies using the above equations as follows, Bilgen (2000):

$$\varepsilon = \frac{\eta}{\varepsilon_f}\left[\frac{r_{ph}+\varepsilon_p}{1+r_{ph}}\right] \qquad (6.9)$$

Two Case Studies corresponding to Figures 6.1 and 6.3 were considered in detail, and in both cases, natural gas was used as fuel. Plant capacity factor was assumed to be 80%. The data for Case Study I appear in Table 6.2 for base-load gas turbine at ISO conditions of 288 K and 101.325 kPa, and 60% relative humidity and they are from a case study earlier reported for an industrial gas turbine (the GE LM2500PE reported by Rice (1987) and Huang (1990). Other parameters employed in the Case Study are isentropic efficiencies of compressor and turbine of 70.4% and 92.6% respectively; intake air temperature same as ISO condition of 288K; process steam is saturated at 2026 kPa; temperature of condensate return is 373 K; and the pinch point temperature difference is 50 K. Bilgen calculated the composition of the products of combustion of natural gas with 226% air (in moles) as follows:

1 CO_2; 0 CO; 2 HO_2; 0.001 OH; 0 NO_2; 0 NO; 24.515 N_2; 4.52 O_2. He also presented the following parameters from his study which agreed quite well with those of Rice (1987) and Huang (1990): cycle efficiency, air flow, specific work output, and exhaust temperature compared quite well with Rice (1987) and fuel utilization efficiency, exergy efficiency, and power-to-heat ratio compared quite well with Huang (1990).

Turbine shaft work (kW)	22007.0
Cycle efficiency (%)	37.0
Cycle pressure ratio	18.7
Air mass flow rate (kg/s)	66.9
Specific work output (kJ/kg air)	328.9
Turbine rotor inlet temperature (K)	1485.0
Exhaust temperature (K)	786.0
Exhaust excess air (%)	226.0
Compressor isentropic efficiency (%)	70.4
Turbine isentropic efficiency (%)	92.6

Table 6.2. Base-load gas turbine data for Case Study I of Bilgen (2000).

The cycle efficiency of 37.62% in Table 6.3 below is for the gas turbine without cogeneration while the fuel efficiency of 77.02% in the same Table 6.3 is for the cogeneration system. This implies a 105% efficiency improvement. The exergy efficiency of the cogeneration system is 50.06% while Bilgen reports an exergy efficiency of only 35.78% for the system without cogeneration, yielding a 40% improvement.

Comparison with the reported data for GE, LM2500PE turbine cited in [4,5] and this study

	Ref. [4]	Ref. [5]	This study
Cycle efficiency (%)	37.00		37.62
Air mass flow rate (kg/s)	66.90		66.33
Specific work output (kJ/kg air)	328.90		331.66
Exhaust temperature (K)	786.15		786.15
Fuel-utilization efficiency (%)		77.00	77.02
Exergy efficiency (%)		52.00	50.06
Power-to-heat ratio		0.92	0.93

Table 6.3. Comparison of the results of Bilgen (2000) with those of Rice (1987) and Huang (1990).

Process heat results of Bilgen (2000) appear in Table 6.4 below.
Fig. 6.4 below shows the 1st law and exergy (2nd law) efficiency and % steam extraction as a function of power-to-heat ratio. The trends of the 1st and 2nd law efficiencies in the figure are quite consistent with equations 6.1, 6.2, and 6.8b. The slow variation of the second law efficiency with power-to-heat ratio indicates that the exergy content of the steam plus power generated from the steam turbine is little degraded.

Process heat results

	Case (i)	Case (ii)
Process steam temperature (K)	486.19	686.15
Saturation temperature of steam (K)	486.19	486.15
Pinch point temperature (K)	536.19	536.19
Process heat produced (kJ/kg air)	358.28	179.16
Specific steam flow rate (kg/kg air)	0.151	0.120
Steam mass flow rate (kg/s)	10.02	3.98
Exergy of process heat (kJ/kg air)	132.37	57.71
Exergy factor of process heat	0.37	0.32
Temperature of extracted steam (K)		599.59
Pressure at steam turbine outlet (kPa)		4.00
Specific work of steam turbine (kJ/kg air)		66.92
Steam turbine shaft work		4440.00

Table 6.4. Process heat results of Bilgen (2000).
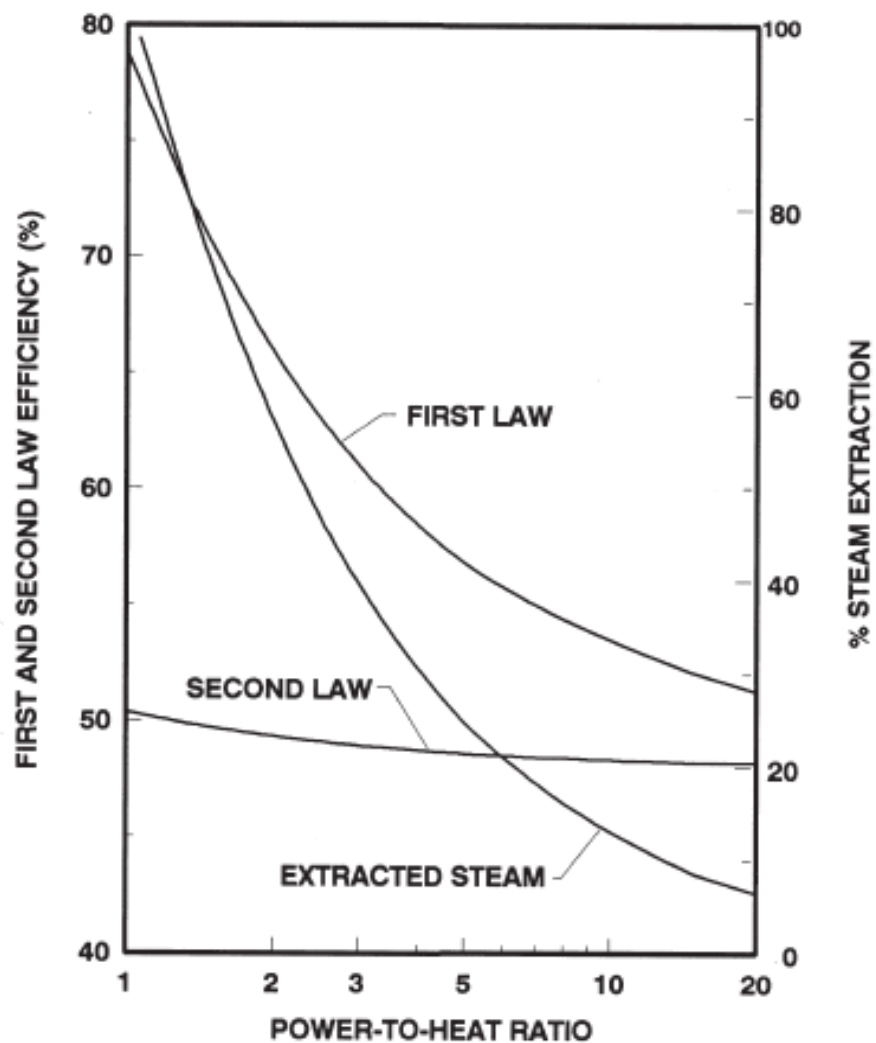
Fig. 6.4. shows the 1st law and exergy (2nd law) efficiency and % steam extraction as a function of power-to-heat ratio.

Similarly, Fig. 6.5 shows power from the steam turbine, total power, process heat production and payback period as a function of the power-to-heat ratio. The process steam production (in t/h) follows the same relationship as that of the % steam extraction in Fig. 6.4.
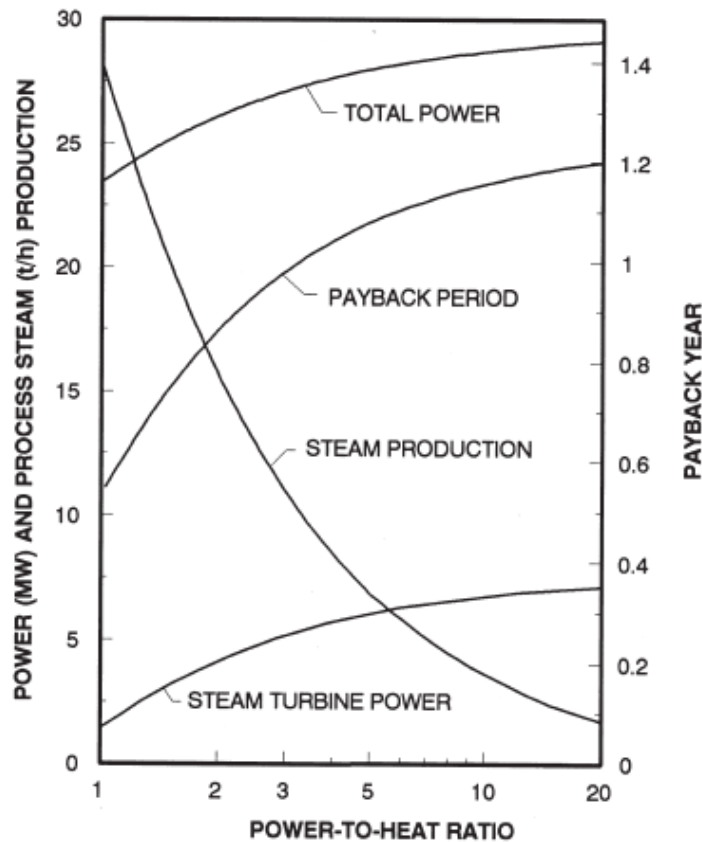

Fig. 6.5. Total power, steam turbine power, process heat production and payback period as a function of the power-to-heat ratio.

Exergy analysis of integrated gasification combined cycle gas turbine (IGCC) plants

Integrated Gasification Combined Cycle (IGCC) plants, as distinct from the general Combined Cycle/Cogeneration plants, have an integrated fuel production unit (gasifier) which provides the fuel (normally gaseous) required by the gas turbine combustors. The feed into the gasifier could be a solid hydrocarbon (usually coal) or biomass (e.g. agricultural wastes, lignocellulosic plants, etc.) as earlier noted in the section on Conventional and New Environmental-conscious Aero and Industrial Gas Turbine Fuels. A schematic of a coal-fired gasifier in an integrated coal gasification combined cycle gas turbine plant (ICGCC) plant appears in Fig. 6.XXX below.

We shall consider a biogas-fired integrated gasification steam-injected gas turbine (BIG/STIG) plant studied by Fagbenle et al. (2007) and shown schematically in Fig. 6.6 below. The Energy Utilization Diagram (EUD) popularized by the Ishida group and discussed in section 6 of this chapter was used to highlight the exergy losses in the various sub-systems of the plant. The EUD is a useful tool for exergy analysis of chemical processes and plants in which the energy level or availability factor (A) is plotted against the energy-transformation quantity (AH), enabling easy identification of subsystems with potentials for performance improvement.
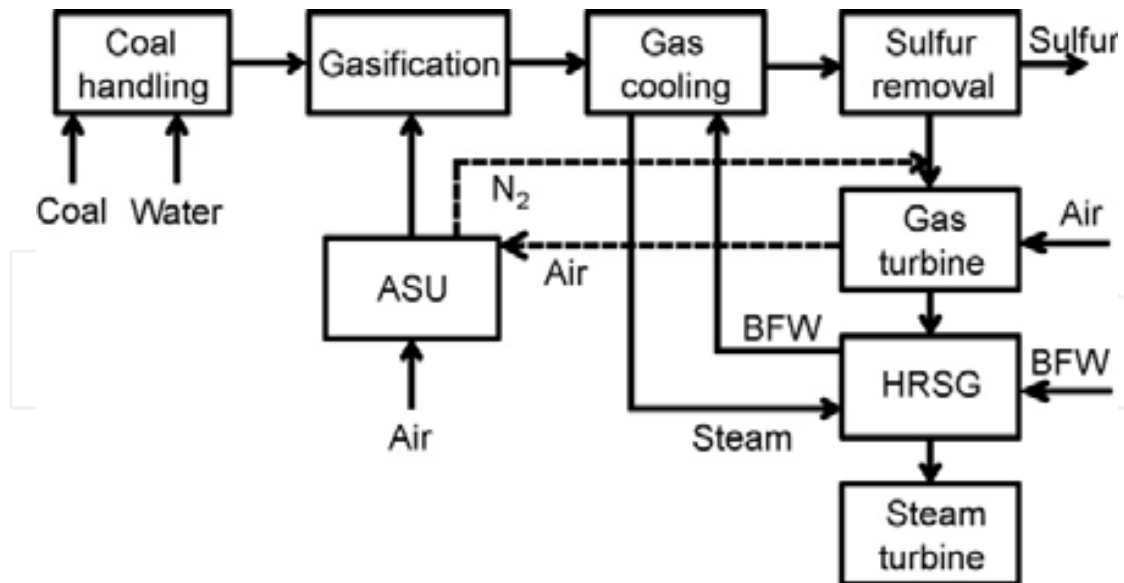
Fig. 6.XXX. Simplified diagram of an integrated coal gasification combined cycle (ICGCC) gas turbine plant. From Emun et al. (2010).

The BIG/STIG plant of Fig. 6.6 consists of a 53 MW gas turbine plant fuelled by fuel gas (syngas assumed to be largely CH_4) from a biogas gasifier and gas clean-up system. The adiabatic combustion temperature was found from the 1st Law to be 1895K but a more realistic (from metallurgical standpoint) turbine inlet temperature (TIT) of 1450 K was used in the analysis. The turbine exhausts at 410 °C (TET) into a Heat Recovery Steam Generator (HRSG) which produces steam for three purposes: injection steam into the turbine for blade cooling, injection steam into the combustor for NOx emission reduction, and blast steam required by the gasifier chemical process. The stack gases exhaust into the atmosphere at 151°C. Air flow of 141 kg/s and at 32.2 bar leaves the compressor, out of which 131.9 kg/s is fed into the combustor while the remaining 9.1 kg/s is fed into the gasifier.

Basis of the Energy Utilization Diagram

The exergy change $\Delta\varepsilon_i$ over all the energy donors and acceptors "i" in the energy-transformation system is:

$$\sum_i \Delta\varepsilon_i = \sum_i (\Delta H_i - T_0 \Delta S_i) \tag{6.10}$$

By the 1st law of thermodynamics, the first term on the RHS of the above equation is zero, since the energy released by the energy donor must equal that gained by the energy acceptor. Also, by the 2nd law of thermodynamics, to total entropy change in the system must be greater than or equal to zero, the equality being for isentropic (lossless) processes, i.e.

$$\sum_i \Delta S_i \geq 0 \tag{6.11}$$

Hence,

$$\sum_i \Delta\varepsilon_i = -T_o \sum_i \Delta S_i \tag{6.12}$$

The availability-factor or the energy level (an intensive parameter) is defined by
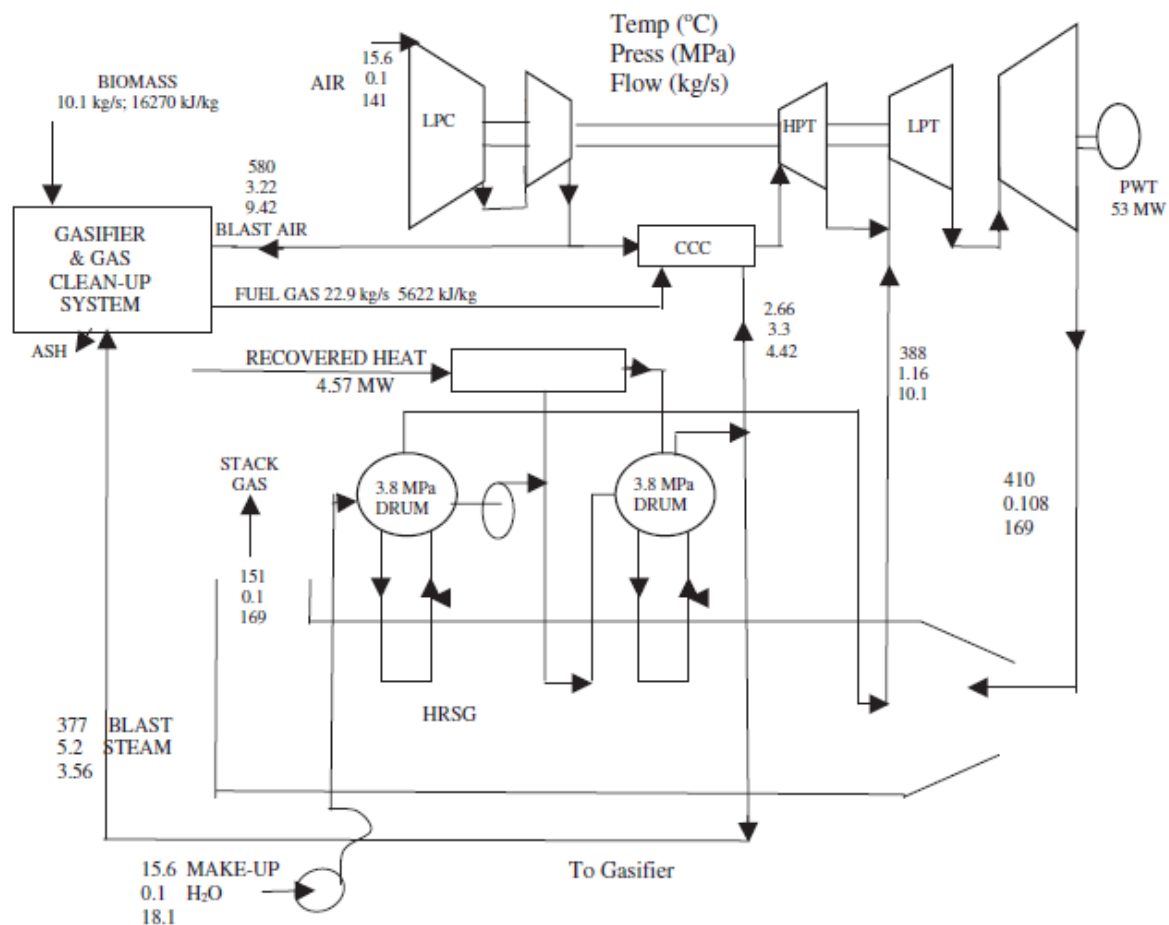
Fig. 6.6. BIG/STIG based on GE LM 5000 aero-derivative gas turbine [Williams (1988)].

$$A = \frac{\Delta \varepsilon}{\Delta H} = 1 - T_0 \frac{\Delta S}{\Delta H} \tag{6.13}$$

It is seen that the relationship between the availability-factor of energy donors and energy acceptors is $A_{ed} \geq A_{ea}$ since in the energy change of the acceptor process, $\Delta H_{ea} > 0$. The exergy loss in the system is thus given by

$$-\sum \Delta \varepsilon_i = \sum_i \Delta H_{ea}(A_{ed} - A_{ea}) \geq 0 \tag{6.14}$$

which, in the limit, gives the system exergy loss as:

$$-\sum \Delta \varepsilon_i = \int_0^{H_{ea}} (A_{ed} - A_{ea})dH_{ea} \tag{6.15}$$

A plot of the energy level of the energy donating process (A_{ed}) and the energy accepting process (A_{ea}) against the transformed energy (ΔH_{ea}) gives the energy loss in the system as the area between the curves of A_{ed} and A_{ea}.   This is the EUD diagram and the energy level difference ($A_{ed} - A_{ea}$) is indicative of the driving force for the energy transformation process. A summary of the operating conditions together with the results of the 1st law efficiencies appears in Table 6.5 below, assuming compressor and turbine isentropic efficiencies of 98% each. The first law efficiency based on power production alone is 41.5% while it is 45% based on both heat and power.

Summary of operating conditions and first law efficiencies of the BIG/STIG plant

Flow rates, kg/s	
Air to combustion chamber	131.9
Air to gasifier	9.1
Fuel gas	22.9
Air/fuel ratio kg_{air}/kg_{fuel}	5.76
Steam injected to combustion chamber	4.42 @ 256 °C
Steam injected to turbine	10.1 @ 388 °C
Fuel subsystem	
Fuel type: fuel gas from biomass gasifier NCV, kJ/kg	5622
Power subsystems	
$\eta_{isen,compressor}$	0.98
$\eta_{isen,turbine}$	0.98
LP & HP compressor, MW	85.0
HP turbine, MW	50.0
LP & Power turbine	93.0
Net generated power (NGP)	53.4
Efficiency (power-based) η_{th}, %	41.5
Efficiency, (power and heat based) η_{th}, %	45.0
Gasifier	
kg fuel-gas/kg biomass	2.27
Blast steam, kg/s	3.56

Table 6.5.

2nd Law or Exergy Analysis and synthesis

Irreversibilities in the turbines and the compressors processes.
The processes through the 2 stages each of the turbines (LP & HP) and the compressors (LP & HP) as well as that through the power turbine (PT) are done irreversibly, and their irreversibilities are
For the turbines:

$$I_t = (1 – \eta_t)W_{HPT,LPT\,\&\,PT} = (1 – 0.98)(143) = 2.9 \text{ MW}$$

For the compressors:

$$I_c = I_c = (\frac{1}{\eta_c} - 1)W_{LPC\&HPC} = 1.7\,MW$$

The gross power input to the compressors is therefore $W_{gross,c}$ = 85 + 1.73 = 86.7 MW, while the net generated power is $W_{net,\,generated}$ = 140.14 - 86.73 = 53.4 MW.
Irreversibility due to the discharge of hot combustion products at 151°C and 1 bar into the environment is given by $I_{exh} = \varepsilon_{stack\,gases}$ = 3.6 MW as detailed below:

Gas	Exergy loss, MW
N_2	2.28
CO_2	0.148
CO	0.278
H_2O	0.860

The Heat Recovery Steam Generator, HRSG

The pinch point on the heat donor side is 546 K and on 512 K on the acceptor side, giving AT_{pinch} = 34°C, while the irreversibility was found to be I_{HRSG} = 7.7 MW.

Combustion chamber subsystem reaction

The total exergy loss in the combustion chamber, I_{cc}, assuming the steam is not dissociated, is given by

$$I_{cc} = \varepsilon_{fuel} - \Delta\varepsilon_{air} - \Delta\varepsilon_{steam}$$

Assuming that the ratio φ of the specific chemical exergy of the fuel to its net calorific value is 0.98, then

$$Icc = (0.98)(5622kJ/kg)(22.9 \ kg/s) - \Delta\varepsilon_{air} - \Delta\varepsilon_{steam}$$

$$= 126.17 - 58.4 - 7$$

$$= 60.8 \ MW$$

It is seen that the exergy loss in the combustion chamber (60.8 MW) is about 49% of the fuel exergy (126.17 MW). Table 6.6 summarizes the results.

Net generated power	53.4 MW		
Exhaust temperature	151 °C		
Pinch point	273 °C		
Minimum ΔT	34 °C		
Location	Exergy Loss (MW)	Fuel exergy, %	Total exergy loss, %
Total exergy loss	76.7	60.8	1000
HRSG	7.7	6.1	10.1
Combustion chamber	60.8	48.2	79.3
Stacks exhaust gases	3.6	2.9	4.7
Turbines	2.9	2.3	3.8
Compressors	1.7	1.3	2.2

Table 6.6. Summary of the net generated power and the exegy loss (Irreversibilities) in the BIG/STIG plant.

The Energy Utilization Diagrams (EUDs) for the combustion chamber and the HRSG

The EUD for the combustion chamber and the HRSG appear in Figs. 6.7 and 6.8 respectively. The largest single subsystem exergy loss occurs in the combustion chamber, being about 79% of the total system exergy loss. The EUD for the HRSG indicates a pinch point of 273°C on the heat donor side and a ΔT = 34°C. The cross-hatched area approximately equals the calculated values shown in Table 6.6.

The irreversibility of the combustion process can be reduced by reducing the effective temperature difference across which the heat transfer is taking place, i.e. between the acceptor and the donor. In this case, preheating the reactants with the exhaust stack gases would reduce the irreversibility of the combustion process. Both the energy and the exergy in the stack gases in this case are both lost. Exergy loss associated with the steam injection mixing process in the combustion chamber has not been taken into consideration, primarily because the amount of steam injected is relatively small.
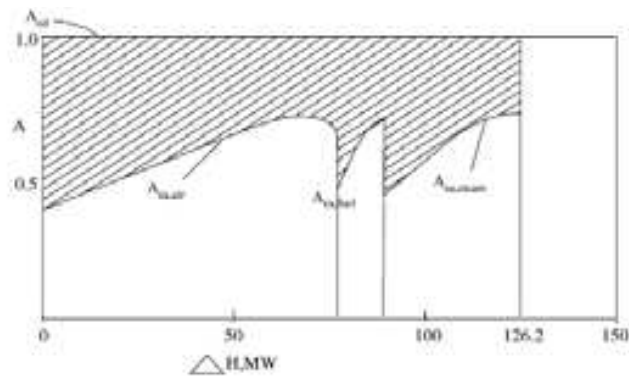
Fig. 6.5. Energy-utilization for the combustion chamber.
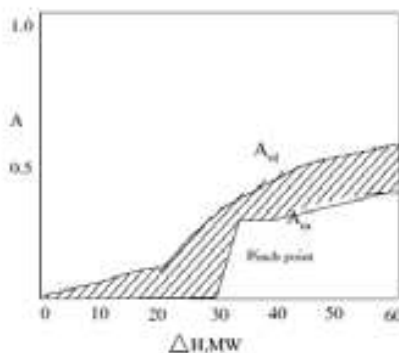
Fig. 6.6. Energy-utilization diagram for the heat recovery steam generator (HRSG).

7. References

Emun, F., Gadalla, M., Majozi, T. and Boer, D. (2010). Integrated gasification combined cycle simulation and optimization. Computers and Chemical Engineering, 34 (2000) 331-338.

Fagbenle, R. Layi, Oguaka, A.B.C., Olakoyejo, O.T. (2007). A thermodynamic analysis of a biogas-fired integrated gasification steam injected gas turbine (BIG/STIG) plant. Applied Thermal Engineering 27 (2007) 2220-2225.

Woudstra, N., Woudstra, T., Pirone, A. and van der Stelt, T. (2010). Thermodynamic evaluation of combined cycle plants. Energy Conversion and Management 51 (2010) 1099-1110.

IPIECA Workshop (2004), Baltimore, USA, 12-13 October 2004.

Rail Transport and Environment – Facts and Figures, Nov. 2008.

Airline Industry Information, May 3, 2010.

The Seattle Times, Dec. 31, 2008.

Shepherd, D. G. Introduction to the Gas Turbine, D. van Nostrand Co. Inc. 1949.

Eastop, T. D. and McConkey, A. Applied Thermodynamics for Engineering Technologists. 2nd. Ed. Longmans, London. 1970.

Wikipedia, Typical specifications for Jet A-1 Aircraft Fuels. 2010.

Specifications for Fuel Gases for Combustion in Heavy-Duty Gas Turbines. GE Power Systems, GEI 41040G, Revised Jan. 2002.

Chris Lewis, (2006). A gas turbine manufacturer's view of Biofuels. Ppt presentation, Rolls Royce plc.

Balat., M., Balat, M., Kirtay, E. and Balat, H. (2009). Main routes for the thermo-conversion of biomass into fuels and chemicals. Part I: Pyrolysis systems. Energy Conversion and Management 50 (2009) 3147-3157.

Balat., M., Balat, M., Kirtay, E. and Balat, H. (2009). Main routes for the thermo-conversion of biomass into fuels and chemicals. Part 2: Gasification systems. Energy Conversion and Management 50 (2009) 3158-3168.

Balat., M. and Balat, H. (2009). Recent trends in global production and utilization of bio-ethanol fuel. Applied Energy 86 (2009) 2273-2282.

Balat., M. and Balat, H. (2010). Progress in biodiesel processing. Applied Energy 87 (2010) 1815-1835.

Baratieri, M., Baggio, P., Fiori, L. and Grigiante, M. (2008). Biomass as an energy source: Thermodynamic constraints on the performance of the conversion process. Bioresource Technology 99 (2008) 7063-7073).

Navarro, X. (2008). Ethanol-powered gas turbine to generate electricity. RSS Feed. Feb. 17th 2008.

C. D. Bolszo and V. G. McDonell, Emissions optimization of a biodiesel fired gas turbine, Proceedings of the Combustion Institute, Vol 32, Issue 2, 2009, Pages 2949-2956.

Pierre A. Glaude, Rene Fournet, Roda Bounaceur and Michel Moliere, (2009). Gas Turbines and Biodiesel: A clarification of the relative NOx indices of FAME, Gasoil and Natural Gas.

Haywood, R. W. Analysis of Engineering Cycles. 2nd edition (SI Units). Pergamon Press. 1975.

Severns, W. H., Degler, H. E. and Miles, J. C. (1964). Steam, Air and Gas Power by Severns, John Wiley, 5th ed. 1964.

Frank J. Brooks, (2000) GE Gas Turbine Performance Characteristics, GER-3567H. GE Energy Services, Atlanta, GA, USA. March 2001.

Pavri, R. and Moore, G. D., Gas Turbine Emissions and Control. GER4211. GE Energy Services, Atlanta, GA. USA. March 2001.

Dincer, I. and Rosen, M. A. Exergy, Energy, Environment and Development, Elsevier. 2007.

Bilgen, E. (2000). Exergetic and engineering analyses of gas turbine based cogeneration systems. Energy 25 (2000) 1215-1229.

Williams, R. H. (1992). Renewable energy on a large scale. In P. E. Trudeau, ed. Energy for a Habitable World, A Call for Action. Crane Russak, New York.

Srinophakun, T., Laowithayangkul, S. and Ishida, M. (2001). Simulation of power cycle with energy utilization diagram. Energy Conversion and Management 42 (2001) 1437-1456.

Khaliq, A. and Kaushik, S. C. (2004). Thermodynamic performance evaluation of combustion gas turbine cogeneration system with reheat. Applied Thermal Engineering 24 (2004) 1785-1795.

Khaliq, A. and Kaushik, S. C. (2004). Second-law based thermodynamic analysis of Brayton/Rankine combined power cycle. Applied Energy 78 (2004) 179-197.

Khaliq, A. (2009). Exergy analysis of gas turbine trigeneration system for combined production of power, heat and refrigetation. International Journal of Refrigeration 32 (2009) 534-545.

Karellas, S., Karl, J. and Kakara, E. (2008). An innovative biomass gasification process and its coupling with microturbine and fuel cell systems. Energy 33 (2008) 284-291.

Ertesvag, I, Kvamsdal, H. M. and Bolland, O. (2005). Exergy analysis of a gas-turbine combined-cycle power plant with precombustion CO_2 capture. Energy 30 (2005) 5-39.

Song, T. W., Sohn, J. L., Kim, T. S. and Ro, S. T. (2006). Performance characteristics of a MW-class SOFC/GT hybrid system based on a commercially available gas turbine. Journal of Power Sources 158 (2006) 361-367.

Ordorica-Garcia, G., Douglas, P., Croiset, E. and Zheng, L. (2006). Technoeconomic evaluation of IGCC power plants for CO_2 avoidance. Energy Conversion and Management 47 (2006) 2250-2259.

Gas Turbines

Edited by Gurrappa Injeti

This book is intended to provide valuable information for the analysis and design of various gas turbine engines for different applications. The target audience for this book is design, maintenance, materials, aerospace and mechanical engineers. The design and maintenance engineers in the gas turbine and aircraft industry will benefit immensely from the integration and system discussions in the book. The chapters are of high relevance and interest to manufacturers, researchers and academicians as well.

How to reference

In order to correctly reference this scholarly work, feel free to copy and paste the following:

Richard 'Layi Fagbenle (2010). Exergy and Environmental Considerations in Gas Turbine Technology and Applications, Gas Turbines, Gurrappa Injeti (Ed.), ISBN: 978-953-307-146-6, InTech, Available from: http://www.intechopen.com/books/gas-turbines/exergy-and-environmental-considerations-in-gas-turbine-technology-and-applications

INTECH
open science | open minds